2019

Global spatial risk assessment of sharks under the footprint of fisheries

Nuno Queiroz

Bradley M. Wetherbee
University of Rhode Island, wetherbee@uri.edu

et al

Citation/Publisher Attribution

Queiroz, N., Humphries, N.E., Couto, A. *et al.* Global spatial risk assessment of sharks under the footprint of fisheries. *Nature* 572, 461–466 (2019). https://doi.org/10.1038/s41586-019-1444-4
Available at: https://doi.org/10.1038/s41586-019-1444-4

Global spatial risk assessment of sharks under the footprint of fisheries

Nuno Queiroz[1,2], Nicolas E. Humphries[2], Ana Couto[1], Marisa Vedor[1], Ivo da Costa[1], Ana M. M. Sequeira[3,4], Gonzalo Mucientes[1], António M. Santos[1], Francisco J. Abascal[5], Debra L. Abercrombie[6], Katya Abrantes[7], David Acuña-Marrero[8], André S. Afonso[9], Pedro Afonso[10,11,12], Darrell Anders[13], Gonzalo Araujo[14], Randall Arauz[15], Pascal Bach[16], Adam Barnett[7], Diego Bernal[17], Michael L. Berumen[18], Sandra Bessudo Lion[19], Natalia P. A. Bezerra[9], Antonin V. Blaison[16], Barbara A. Block[20], Mark E. Bond[21], Russell W. Bradford[22], Camrin D. Braun[23], Edward J. Brooks[24], Annabelle Brooks[24,25], Judith Brown[26], Barry D. Bruce[22], Michael E. Byrne[27], Steven E. Campana[28], Aaron B. Carlisle[29], Demian D. Chapman[21], Taylor K. Chapple[20], John Chisholm[30], Christopher R. Clarke[31], Eric G. Clua[32], Jesse E. M. Cochran[18], Estelle C. Crochelet[33,34], Laurent Dagorn[16], Ryan Daly[35], Daniel Devia Cortés[36], Thomas K. Doyle[37,38], Michael Drew[39], Clinton A. J. Duffy[40], Thor Erikson[41], Eduardo Espinoza[42], Luciana C. Ferreira[43], Francesco Ferretti[20], John D. Filmalter[16,44], G. Chris Fischer[45], Richard Fitzpatrick[7], Jorge Fontes[10,11,12], Fabien Forget[16], Mark Fowler[46], Malcolm P. Francis[47], Austin J. Gallagher[48,49], Enrico Gennari[44,50,51], Simon D. Goldsworthy[52], Matthew J. Gollock[53], Jonathan R. Green[54], Johan A. Gustafson[55], Tristan L. Guttridge[56], Hector M. Guzman[57], Neil Hammerschlag[49,58], Luke Harman[37], Fábio H.V. Hazin[9], Matthew Heard[39], Alex R. Hearn[59], John C. Holdsworth[60], Bonnie J. Holmes[61,62], Lucy A. Howey[63], Mauricio Hoyos[64], Robert E. Hueter[65], Nigel E. Hussey[66], Charlie Huveneers[39], Dylan T. Irion[67], David M.P. Jacoby[68], Oliver J. D. Jewell[69,70], Ryan Johnson[71], Lance K. B. Jordan[63], Salvador J. Jorgensen[72], Warren Joyce[46], Clare A. Keating Daly[35], James T. Ketchum[64], A. Peter Klimley[73], Alison A. Kock[44,74,75,76], Pieter Koen[77], Felipe Ladino[19], Fernanda O. Lana[78], James S.E. Lea[31], Fiona Llewellyn[53], Warrick S. Lyon[47], Anna MacDonnell[46], Bruno C. L. Macena[9,11], Heather Marshall[17,79], Jaime D. McAllister[80], Rory

McAuley[81], Michael A. Meÿer[13], John J. Morris[64], Emily R. Nelson[49], Yannis P. Papastamatiou[21], Toby A. Patterson[22], Cesar Peñaherrera-Palma[82,83], Julian G. Pepperell[84], Simon J. Pierce[85], Francois Poisson[16], Lina Maria Quintero[19], Andrew J. Richardson[86], Paul J. Rogers[52], Christoph A. Rohner[85], David R.L. Rowat[87], Melita Samoilys[88], Jayson M. Semmens[80], Marcus Sheaves[7], George Shillinger[20,83,89], Mahmood Shivji[27], Sarika Singh[13], Gregory B. Skomal[30], Malcolm J. Smale[90], Laurenne B. Snyders[13], German Soler[19], Marc Soria[16], Kilian M. Stehfest[80], John D. Stevens[22], Simon R. Thorrold[91], Mariana T. Tolotti[16], Alison Towner[70,92], Paulo Travassos[9], John P. Tyminski[65], Frederic Vandeperre[10,11,12], Jeremy J. Vaudo[27], Yuuki Y. Watanabe[93], Sam B. Weber[94], Bradley M. Wetherbee[27,95], Timothy D. White[20], Sean Williams[24], Patricia M. Zárate[96], Robert Harcourt[97], Graeme C. Hays[98], Mark G. Meekan[43], Michele Thums[43], Xabier Irigoien[99], Victor M. Eguiluz[100], Carlos M. Duarte[18], Lara L. Sousa[2], Samantha J. Simpson[2,101], Emily J. Southall[2] & David W. Sims[2,101,102]*

1 Centro de Investigação em Biodiversidade e Recursos Genéticos/Research Network in Biodiversity and Evolutionary Biology, Campus Agrário de Vairão, Universidade do Porto, 4485-668 Vairão, Portugal

2 Marine Biological Association of the United Kingdom, The Laboratory, Citadel Hill, Plymouth PL1 2PB, UK

3 UWA Oceans Institute, Indian Ocean Marine Research Centre, University of Western Australia, Crawley, WA 6009, Australia

4 School of Biological Sciences, University of Western Australia, Crawley, WA 6009, Australia

5 Spanish Institute of Oceanography, Vía Espaldón, Dársena Pesquera PCL8, 38180 Santa Cruz de Tenerife, Spain

6 Abercrombie and Fish, 14 Dayton Avenue, Port Jefferson Station, NY 11776, USA

7 College of Science and Engineering, James Cook University, Cairns, QLD, Australia

8 Institute of Natural and Mathematical Sciences, Massey University, New Zealand

9 UFRPE (Universidade Federal Rural de Pernambuco), Departamento de Pesca e Aquicultura, Rua Dom Manoel de Medeiros, s/n, 52171-900, Recife- PE, Brazil

10 MARE, Laboratório Marítimo da Guia, Faculdade de Ciências da Universidade de Lisboa, Av. Nossa Senhora do Cabo, 939, 2750-374 Cascais, Portugal

11 IMAR – Institute of Marine Research, Departamento de Oceanografia e Pescas, Universidade dos Açores, Horta, Portugal

12 Okeanos - Departamento de Oceanografia e Pescas, Universidade dos Açores, Horta, Portugal

13 Department of Environmental Affairs, Oceans and Coasts Research, P.O. Box 52126, Victoria & Alfred Waterfront, Cape Town 8001, South Africa

14 Large Marine Vertebrates Research Institute Philippines, Cagulada Compound, Tejero, Jagna, 6308, Bohol, Philippines

15 Asociación CREMA / Fins Attached / Migramar, Guanacaste Province, San Francisco de Coyote, Costa Rica

16 Institut de Recherche pour le Développement, UMR MARBEC (IRD, Ifremer, Univ. Montpellier, CNRS), Sète, France

17 University of Massachusetts Dartmouth, Biology Department, Dartmouth, MA, USA

18 Red Sea Research Center, Division of Biological and Environmental Science and Engineering, King Abdullah University of Science and Technology, Thuwal, 23955, Kingdom of Saudi Arabia

19 Fundación Malpelo y Otros Ecosistemas Marinos, Carrera 11 # 87 - 51 Local 4 Piso 2, Bogota, Columbia

20 Hopkins Marine Station of Stanford University, 120 Oceanview Blvd., Pacific Grove, CA 93950, USA

21 Department of Biological Sciences, Florida International University, 3000 NE 151st Street, North Miami, FL 33181 USA

22 CSIRO Oceans and Atmosphere, GPO Box 1538, Hobart, Tas 7000, Australia

23 Massachusetts Institute of Technology-Woods Hole Oceanographic Institution Joint Program in Oceanography/Applied Ocean Science and Engineering, Cambridge, MA USA

24 Shark Research and Conservation Program, Cape Eleuthera Institute, Eleuthera, The Bahamas

25 University of Exeter, Prince of Wales Road, Exeter, EX4 4PS, UK

26 South Atlantic Environmental Research Institute, Stanley Cottage, FIQQ 1ZZ, Falkland Islands

27 Department of Biological Sciences, The Guy Harvey Research Institute, Nova Southeastern University, Dania Beach, FL, USA

28 Life and Environmental Sciences, University of Iceland, Reykjavik, Iceland

29 University of Delaware, School of Marine Science and Policy, 700 Pilottown Rd., Lewes, DE 19958, USA

30 Massachusetts Division of Marine Fisheries, New Bedford, MA USA

31 Marine Research Facility, Jeddah, Saudi Arabia

32 PSL, Labex CORAIL, CRIOBE USR3278 EPHE-CNRS-UPVD, PoBox 1013, 98729 Papetoai, French Polynesia

33 Agence de Recherche pour la Biodiversité à la Réunion (ARBRE), Réunion, France

34 Institut de Recherche pour le Développement, UMR 228 ESPACE-DEV, Réunion, France

35 Save Our Seas Foundation – D'Arros Research Centre (SOSF-DRC), Rue Philippe Plantamour 20,CH-1201 Geneva, Switzerland

36 Department of Fisheries Evaluation, Fisheries Research Division, Instituto de Fomento Pesquero (IFOP), Blanco 839, Valparaíso 2361827, Chile

37 School of Biological, Earth and Environmental Sciences, University College Cork, Ireland

38 MaREI Centre, Environmental Research Institute, University College Cork, Ireland

39 School of Biological Sciences, College of Science and Engineering, Flinders University, GPO Box 2100, Adelaide, SA, Australia

40 Department of Conservation, Private Bag 68908, Auckland, New Zealand

41 South African Institute for Aquatic Biodiversity, Geological Sciences, UKZN, Durban, 4001, South Africa

42 Dirección Parque Nacional Galapagos / MigraMar, Galapagos Islands, Ecuador

43 Australian Institute of Marine Science, Indian Ocean Marine Research Centre (UWA), 35 Stirling Hwy, Crawley 6009 WA, Australia

44 South African Institute for Aquatic Biodiversity (SAIAB), Private Bag 1015, Grahamstown 6140, South Africa

45 OCEARCH, Park City, Utah 84068, USA

46 Bedford Institute of Oceanography, Dartmouth, NS Canada

47 National Institute of Water and Atmospheric Research, Private Bag 14901, Wellington, New Zealand

48 Beneath the Waves, Herndon, VA, USA

49 Rosenstiel School of Marine and Atmospheric Science, University of Miami, 4600 Rickenbacker Causeway, Miami, FL 33149, USA

50 Oceans Research, PO box 1767, Mossel Bay 6500, South Africa

51 Department of Ichthyology and Fisheries Science, Rhodes University, Grahamstown, South Africa

52 SARDI Aquatic Sciences, Henley Beach, Adelaide, South Australia, 5022, Australia

53 Zoological Society of London, Regent's Park, London, NW1 4RY, UK

54 Galapagos Whale Shark Project, Galapagos Islands, Ecuador

55 Griffith Centre for Coastal Management, Griffith University School of Engineering, Griffith University, Gold Coast, Queensland, 4222, Australia

56 Bimini Biological Field Station, South Bimini, Bahamas

57 Smithsonian Tropical Research Institute, PO Box 0843-03092, Panama, Republic of Panama

58 Abess Center for ecosystem Science and Policy, University of Miami, 1365 Memorial Drive, #230, Coral Gables, FL 33146, USA

59 Galapagos Science Center, Universidad San Francisco de Quito / MigraMar, Quito, Ecuador

60 Blue Water Marine Research, PO Box 402081, Tutukaka, New Zealand

61 Department of Agriculture and Fisheries, 41 George St, Brisbane, Queensland 4000, Australia

62 University of Queensland, St Lucia, Brisbane, Queensland 4001, Australia

63 Microwave Telemetry, Inc., Columbia, MD, USA

64 Pelagios-Kakunja / MigraMar, Cuauhtémoc 155, Pueblo Nuevo, 23060 La Paz, Mexico

65 Mote Marine Laboratory, Center for Shark Research, Sarasota, FL 34236, USA

66 University of Windsor, Biological Sciences, 401 Sunset Avenue, Windsor, Ontario, N9B 3P4, Canada

67 Cape Research and Diver Development, Simon’s Town, South Africa

68 Institute of Zoology, Zoological Society of London, Regent's Park, London, NW1 4RY, UK

69 Centre for Sustainable Aquatic Ecosystems, Harry Butler Institute, Murdoch University, Western Australia

70 Dyer Island Conservation Trust, Kleinbaai, Western Cape, South Africa

71 Blue Wilderness Research, Village Walk, 1 King Shaka Ave, Durban, 4001, South Africa

72 Monterey Bay Aquarium, 886 Cannery Row, Monterey, CA 93940, USA

73 University of California Davis, Davis, CA 95616, USA

74 Cape Research Centre, South African National Parks, South Africa

75 Shark Spotters, P. O. Box 22581, Fish Hoek, 7974, South Africa

76 Institute for Communities and Wildlife in Africa, Department of Biological Sciences, University of Cape Town, Private Bag X3, Rondebosch 7701, South Africa

77 Western Cape Department of Agriculture, Veterinary Services, Private Bag X1, Elsenburg, 7607 South Africa

78 UFF (Universidade Federal Fluminense), Departamento de Biologia Marinha, Rua Alexandre Moura, 24210-200, Niterói- RJ, Brazil

79 Atlantic White Shark Conservancy, Chatham, MA, USA

80 Fisheries and Aquaculture Centre, Institute for Marine and Antarctic Studies , University of Tasmania, Private Bag 49, Hobart, TAS 7001, Australia

81 Department of Fisheries, Government of Western Australia, 39 Northside Dr, Hillarys WA 6025, Australia

82 Pontificia Universidad Católica del Ecuador Sede Manabi, Portoviejo 130103, Ecuador

83 MigraMar, 9255 Sir Francis Drake Boulevard, Olema, CA 94950, USA

84 Pepperell Research & Consulting Pty LTD, PO Box 1475, Noosaville BC, Queensland 4565, Australia

85 Marine Megafauna Foundation, 11260 Donner Pass Road, Truckee, CA 96161, USA

86 Conservation and Fisheries Department, Ascension Island Government, Ascension Island, South Atlantic ASCN 1ZZ

87 Marine Conservation Society Seychelles, PO Box 384, Victoria, Mahe, Seychelles

88 CORDIO, East Africa, PO Box 10135, Mombasa, 80101, Kenya

89 Upwell, 99 Pacific Street, Suite 375-E, Monterey, CA 93940

90 Department of Zoology and Insitute for Coastal and Marine Research, Nelson Mandela University, South Africa

91 Woods Hole Oceanographic Institution, Woods Hole, MA, USA

92 Department of Ichthyology and Fisheries Science, Rhodes University, PO BOX 94, Grahamstown 6140, South Africa

93 National Institute of Polar Research, Tachikawa, Tokyo 190-8518, Japan / SOKENDAI (The Graduate University for Advanced Studies), Tachikawa, Tokyo 190-8518, Japan

94 Centre for Ecology and Conservation, University of Exeter, Penryn Campus, Cornwall TR10 9FE, UK

95 Department of Biological Sciences, University of Rhode Island, Kingston RI, USA

96 Department of Oceanography and Environment, Fisheries Research Division, Instituto de Fomento Pesquero (IFOP), Blanco 839, Valparaíso 2361827, Chile

97 Department of Biological Sciences, Macquarie University, Sydney, NSW2109, Australia

98 School of Life and Environmental Sciences, Deakin University, Geelong, Victoria, Australia

99 AZTI Tecnalia, Herrera Kaia, Portualdea z/g Pasaia Gipuzkoa 20110, Spain

100 Instituto de Fisica Interdisciplinar y Sistemas Complejos, Consejo Superior de Investigaciones Cientificas-University of the Balearic Islands, E-07122 Palma de Mallorca, Spain

101 Ocean and Earth Science, University of Southampton, National Oceanography Centre Southampton,Waterfront Campus, European Way, Southampton SO14 3ZH, UK

102 Centre for Biological Sciences, University of Southampton, Building 85, Highfield Campus, Southampton SO17 1BJ, UK

*e-mail: dws@mba.ac.uk

Industrialised fishing of the high seas (areas beyond national jurisdiction) is a major source of mortality to marine megafauna[1-3]. Effective management and conservation of highly migratory species in the high seas depends on resolving overlap between animal movements and distributions and fishing effort across far-reaching population ranges[4,5]. Yet, this information at a global scale is lacking[1,5,6]. Here we show, based on a unique big-data approach combining satellite-tracked movements of 1,681 pelagic sharks (23 species) and global fishing fleets, that 45% of space used by sharks in an average year falls under the footprint of pelagic longline fisheries, the gear type catching most pelagic sharks[5,6]. Strikingly, monthly shark-longline overlap remained high at 40%, indicating significant overlap in both space and time. Space use hotspots of commercially valuable species had the highest overlap with longlines (80–94%) and were also associated with significant increases in fishing effort and capture-induced shark mortality compared to other species[7,8], either because fisheries directly target sharks or sharks occupy habitats of targeted fish stocks. Protected species within some national jurisdictions and on the high seas overlapped longline fisheries by >80%, emphasising the continued need for management measures that minimise bycatch of the most threatened species. Only a few large-scale hotspots of shark distribution occurred in areas generally free from industrial fishing, with some typically associated with effective local management. We conclude that pelagic sharks have limited spatial refuges from current levels of fishing effort on the high seas. These results demonstrate an urgent need for conservation measures at high-seas shark hotspots and highlight the potential of simultaneous satellite surveillance of megafauna and fishers as a tool for near–real time, dynamic management of marine megafauna.

Humans have hunted large marine animals (marine megafauna) in open oceans for at least 42,000 years[9], however only since the 1950s have the international fishing fleets that target

large, epipelagic fishes spread into the high seas[10]. Prior to this, highly mobile fishes occupying this environment inhabited a spatial refuge largely free from exploitation, since fishing mostly concentrated on continental shelves[3,10]. Of the fishes occupying the high seas, pelagic sharks' movements will likely have a strong impact on their vulnerability to fishing pressure: they are among the widest–ranging of vertebrates, with some species exhibiting annual ocean-basin-scale migrations[11], long term trans-ocean movements[12], and/or fine-scale site fidelity to preferred shelf and open ocean areas[5,11,13]. These species account for ~50% of all identified shark catch worldwide in target fisheries or as bycatch[14]. Regional declines in abundance of pelagic sharks have been reported[15,16], but it is unclear whether exposure to high fishing effort extends across ocean-wide population ranges and overlaps areas in the high seas where sharks are most abundant[5,15]. Conservation of pelagic sharks – which currently have limited high seas management[14,17,18] – would benefit greatly from a clearer understanding of the spatial relationships between sharks' preferred habitats and active fishing zones. However, obtaining unbiased estimates of shark and fisher distributions is complicated by the fact that most data on pelagic sharks comes from catch records and other fisheries-dependent sources[17,18].

Here, we provide the first global estimate of the extent of space use overlap of marine vertebrates with industrial fisheries. This is based on the analysis of the movements of pelagic sharks tagged with satellite transmitters in the Atlantic, Indian and Pacific oceans, together with fishing vessels monitored globally by the automatic identification system (AIS), developed as a vessel safety and anti-collision system (see Methods). Our study focused on 23 species of large pelagic sharks (median maximum total body length = 3.7 m) that occupy oceanic and/or neritic habitats spanning broad distributions from temperate to tropical waters (Supplementary Table 1). All these species face some level of fishing pressure in coastal, shelf and/or high-seas fisheries, with the International Union for the Conservation of Nature

(IUCN) Red List assessing 26% of the 23 species globally as having 'near threatened' status, 48% as 'vulnerable' and 17% 'endangered' (Supplementary Table 2). Regional fisheries management organizations (RFMOs) are tasked with management of sharks in high seas areas, yet little or no management is in place for the majority of species[3,5,14-20] (Supplementary Table 2).

From 2002–2017 we tagged 1,804 pelagic sharks with satellite transmitters, with 60% of deployments occurring between 2010 and 2017 (Methods; Extended Data Fig. 1, Supplementary Tables 3, 4). Eleven of the largest species/taxa groups accounted for 96% of all tags deployed (blue *Prionace glauca*; shortfin mako *Isurus oxyrinchus*; tiger *Galeocerdo cuvier*; salmon *Lamna ditropis*; whale *Rhincodon typus*; white *Carcharodon carcharias*; oceanic whitetip *Carcharhinus longimanus*; porbeagle *Lamna nasus*; silky *Carcharhinus falciformis*; bull *Carcharhinus leucas*; and hammerhead *Sphyrna* spp. sharks) (Supplementary Table 3). Tracks with daily locations were reconstructed for 1,681 individuals totalling 281,724 tracking days (Methods).

Movement patterns indicated that multiple species aggregated within the same large-scale areas within an ocean (Fig. 1). Species co-occurred in major oceanographic features, such as the Gulf Stream (blue, shortfin mako, tiger, white and porbeagle sharks), the California Current (blue, shortfin mako, white and salmon sharks), and in the East Australian Current (blue, shortfin mako, tiger, white and porbeagle sharks) (Fig. 1, Extended Data Fig. 2; Supplementary Results and Discussion 2.1). The global density map reveals distribution patterns of pelagic sharks and locations of space use hotspots (defined here as those areas with $\geq 75^{th}$ percentile of weighted daily location density). Implementation of a weighted spatial density meant individual location estimates closer to a tagging location received a lower weight than later locations because more sharks had locations earlier in their tracks[13], thus reducing bias (Fig. 2a) (see Methods). Major hotspots of tracked pelagic sharks in the

Atlantic Ocean were in the Gulf Stream and its western approaches, Caribbean Sea, Gulf of Mexico and around oceanic islands such as the Azores (Fig. 2a). In the Indian Ocean, hotspots were evident in the Agulhas Current, Mozambique Channel, the South Australian Basin and northwest Australia, while Pacific hotspots were in the California Current, Galapagos Islands, eastern Equatorial Counter Current, and around New Zealand (Supplementary Table 5). Although tagging sites occurred as expected in some shark space use hotspots – as tagging rates are inherently higher in hotspots – we also identified numerous hotspots where no tagging sites occurred: in the North Atlantic (outer Gulf Stream, Charlie Gibbs Fracture Zone, western European shelf edge and Bay of Biscay); Indian Ocean (Somali Basin, Chagos Archipelago, South Australian Basin); and the Pacific (Alaska Current, outer California Current, white shark 'Café' area[13], North Equatorial Current, northern East Pacific Rise, Isakov/Makarov Seamounts, Chatham Rise) (Extended Data Fig. 1).

To determine the extent to which shark space use hotspots fall under the footprint of global industrialised fisheries we mapped the movements of fishing vessels carrying AIS transmitters, estimated to be fitted on 50–75% of active vessels >24 m length[21]. In the context of monitoring fishing activity, there are known disadvantages of using AIS data[22] compared to vessel monitoring system (VMS) data; for example, longer gaps in data coverage in space and time[23] and the potential for misidentification of fishing activity by different gears[21]. However, given that VMS data is not widely available, the principal advantage of AIS is as a freely available global dataset of fishing activity that provides a useful and valid starting point for investigating the overlap of shark space use by global fisheries. As a first step we mapped the mean annual fishing effort (days) of 83,628 AIS-equipped fishing vessels using various gear types[21] during 2012–2016 (Extended Data Fig. 3; Methods). In addition to using all fishing vessels within the dataset, the estimated global fishing effort of drifting pelagic

longline (n = 5,565) and purse seine vessels (n = 6,941) were mapped separately as these two gears catch the majority of pelagic sharks[14,17] (Fig. 2b; Extended Data Fig. 4).

The global distribution map of all vessels' fishing effort identifies several large–scale, high use areas such as the western European Shelf in the northeast Atlantic, Mediterranean Sea, Patagonian Shelf off Argentina, Peru Current, the Equatorial Pacific region and off China (Extended Data Fig. 3, Supplementary Table 6). There were also areas where industrial fishing activity appeared sparse, for example the central and southwest North Atlantic, northeast Pacific, and northern Indian oceans. To explore the spatial heterogeneities of sharks and vessels we used generalised additive models to determine how shark relative density and fishing effort were affected by environmental covariates (see Methods; Supplementary Table 7). Distributions of pelagic shark density and fishing effort of all vessels, and for pelagic longline vessels separately, were best explained by the same drivers, with all demonstrating strong relationships with habitat types characterised by surface and subsurface temperature gradients (fronts[24]; thermoclines) and/or high primary productivity (Extended Data Table 1, Extended Data Fig. 5). Relative densities of sharks were higher around ocean areas with specific surface (fronts, ~1.0°C/100 km; and mesoscale eddy edges) and subsurface (thermocline, ~40 m) boundary conditions and moderate chlorophyll-*a* concentrations (~0.3 mmol m^{-3}), a proxy for primary productivity. The same set of environmental covariates best explained distributions of shark densities and fishing effort of all vessels and of longlines only (Supplementary Results and Discussion 2.2). This predicts high spatial overlap because sharks are known to aggregate in biologically productive features like fronts to enhance foraging opportunities[5,6,24], a behaviour that fishers exploit to increase their chances of making higher catches of commercially valuable sharks and other epipelagic fishes[5,6]. For pelagic longliners, national fleets that target sharks for fins and meat (or as targeted bycatch) include China, Taiwan, Spain and Portugal[5,14], which comprise 67% of all AIS-tracked

longlining vessels analysed in this study (Extended Data Table 2). Other large national fleets such as the U.S.A., Canada and Japan potentially take shark as unintentional bycatch[17]. Hence, two potential explanations for spatial overlap of sharks and fishing vessels include: (i) fishers track sharks (shark habitats) as target species for valuable fins and, for some species, meat, or (ii) sharks occur in similar habitats as fishers because, for example, they have the same target prey (e.g. tunas, billfishes) or prey on the same species that targeted fish also feed upon (e.g. small-bodied schooling fish).

To quantify the actual shark space use occupied by fishing vessels, as indicated by the modelling, we calculated the mean spatial overlap of tracked sharks with fisheries for a mean year within the datasets (Methods). Overlap was defined as shark and vessel spatial co-occurrence within a 1 × 1° grid cell in an average year, where 1° latitude at the equator (110.6 km) matches the approximate length of high seas longlines, i.e. 100 km long with an average of 1,200 baited hooks[5]. Globally, the distribution of industrial fishing activity of all vessels in the dataset overlapped 81% of the space use of tracked sharks at the 1 × 1° scale (mean overlap = 80.8% ± 29.9 S.D.; median = 96.2%, n = 1,681 tracks). Decreasing grid cell size can reduce percentage spatial overlap estimates[21], however although we found the mean overlap at 0.5 × 0.5° and 0.25 × 0.25° grid cell sizes decreased as expected, it remained relatively high at 67 and 56%, respectively (Extended Data Table 3). However, there were large regions of oceans where no or very few sharks were satellite tracked despite high fishing activity, for example the Patagonian Shelf and in the northwest and southeast Pacific Ocean (Extended Data Fig. 3). The northwest Pacific Ocean supports major global fishing-effort hotspots off China and Japan, yet there were very limited shark tracking data in this region. This suggests that either sharks are already in low abundance such that tagging studies are less viable, or, more likely, that transmitters are not available or data cannot be

354 accessed. This study highlights an urgent need for fishery-independent shark occurrence data,
355 such as from tracking, to underpin spatial risk assessments in global fishing hotspots.

356 We focused our detailed analysis of shark overlap with that of longline fishing effort, as this
357 gear catches most pelagic sharks globally[17] and since most AIS fishing vessel gear types
358 represented in the dataset do not target or bycatch sharks[21]. Where we were able to determine
359 shark space use directly using tags, coverage by fisheries was dominated by pelagic longline
360 gear (Fig. 2a, b). The mean spatial overlap between sharks and longline fishing effort was
361 45% (mean = 44.8% ± 41.4 S.D.; median = 33.7%) at the 1 × 1° grid size (Extended Data
362 Table 2), with the spatial pattern being very similar to that for sharks and all mapped AIS
363 fishing vessels (compare Fig. 2b with Extended Data Fig. 3a). Across four regions where the
364 majority of sharks were tracked, mean spatial overlap of all 11 most frequently tracked
365 species/taxa groups with longline fishing effort ranged from 24% (east Pacific; n = 585
366 tracks) to 55% (north Atlantic; n = 656 tracks) and 66% (Oceania: Australia, New Zealand,
367 southeast Asia; n = 151 tracks), up to 82% for the southwest Indian ocean (n = 114 tracks)
368 (Extended Data Table 4).

369 Hotspots of spatial overlap intensity (see Methods) of sharks and longlines were evident in
370 the Gulf Stream and stretching eastward to the Azores, western European shelf edge, west
371 African upwelling, California Current, east of the Galapagos, Agulhas Current, Seychelles
372 archipelago, the southern Great Barrier Reef, and New Zealand shelf waters (Fig. 2c,
373 Supplementary Table 8). Overlap intensity varied across species and among oceans,
374 reflecting the heterogeneous distributions of space use by sharks and longline fishing activity
375 (Extended Data Fig. 6). For example, spatial overlap of sharks and longline fishing effort,
376 averaged across all oceans, ranged from 92% for the porbeagle, down to 11% for the oceanic
377 whitetip shark. Among oceans, the overlap of space use by blue sharks – the pelagic shark

most commonly caught by open-ocean longline fleets[17] – was 94% in the North Atlantic, decreasing to 34% in the east Pacific.

An important question is whether significant areas of the high seas used by pelagic sharks exist that are largely free from AIS-monitored fishing activity of longline and purse seine vessels as these could be targeted for shark conservation measures. Identifying such areas can only be addressed with the fishery-independent distributions presented here. We found some large–scale areas with low overlap between shark space use and fishing effort, e.g. the central and south-western North Atlantic (Fig. 2a, b; Extended Data Fig. 4). Similarly, the high seas in the northeast Pacific, the South Australian Basin, and some waters between Australia and New Zealand supported space use by sharks but sparse AIS fishing vessel activity. Although it is possible longliners and purse seiners were present but not using AIS, low fishing activity also occurred in many of the territorial waters around oceanic islands in the Atlantic, Indian Ocean and Pacific (Fig. 2b), indicating these zones, some of which are marine protected areas (MPAs), may offer some refuge to sharks from AIS-monitored fishing vessels. For example, the Chagos Archipelago (Indian Ocean) was identified as a shark hotspot even though no sharks were tagged there, with this archipelago lying within one of the world's largest MPAs that has maintained a ban on commercial fishing since 2010. Furthermore, the shark hotspot in the south-western North Atlantic centred in the Caribbean showed very low overlap with AIS vessels, possibly due to the presence of a large MPA (Bahamas) that prohibits pelagic longline fishing[25] or due to few vessels there using AIS. However, a general characteristic of large areas with low longline fishing activity was also one of lower shark densities ($<75^{th}$ percentile of relative density; Fig. 2a), indicating sharks were not remaining in these areas but moving through them, potentially as part of foraging excursions or migrations for reproduction[11,13]. The lower relative density of sharks suggests lower productivity – confirmed by our modelling results (model 1; Extended Data Fig. 5) – and consequently

poorer fishing opportunities, which may explain the low fishing effort. The results also show that very few large hotspots of space use by pelagic sharks occurred in areas free from AIS fishing vessels, particularly longline and purse seine gears (Fig. 2c; Extended Data Fig. 4).

To estimate the potential risk of exposure of sharks in different ocean regions to longline fishing effort, we calculated the fishing effort individual sharks were subjected to on each track day, standardised to account for variations in individual track durations (hereafter termed fishing effort per shark space use) (see Methods). As expected across all oceans and species, longline fishing effort per shark space use was highly variable (mean = 34.7 d ± 125.4 S.D.; median = 8.7 d) (Extended Data Table 3). Given this, we tested whether the mean annual longline fishing effort (2012–2016) overlap with mean annual shark space use (2002–2017) was indicative of actual sharks captured and landed by fisheries. We compared the mean annual longline fishing effort for North Atlantic shark species (the ocean for which we had the most species and tracks) with Food and Agriculture Organization of the United Nations (FAO) officially recorded mean annual North Atlantic landings of those species (2012–2016) (Methods). We found a significant positive relationship between landings and AIS longline effort (linear regression, r^2 = 0.51, n = 9 species or taxa group, F = 7.14, $F_{0.05(1),1,7}$ = 5.59, p = 0.032) (Extended Data Fig. 7), confirming longline fishing effort in shark space use areas reflects major trends in fishing-induced shark mortality.

The extent of spatial overlap between shark distribution and longline fishing effort indicates which species are more exposed to fishing and how this exposure is distributed (Fig. 3). Since actual shark mortality (landings) is related to longline fishing effort in shark space use areas, it follows that sharks exposed to high fishing overlap and effort (greater susceptibility) will be at greater risk of capture than those exposed to low overlap and effort (Fig. 3; Extended Data Table 4). We found the main commercially valuable pelagic sharks were grouped within

the highest potential risk zone in the North Atlantic and east Pacific (blue and shortfin mako sharks), and in the Oceania region (blue shark) (Fig. 3a,b) (see Supplementary Results and Discussion 2.3, 2.4 for significance tests and results for other species). In the North Atlantic, between 79 and 94% of tracked space used by shortfin mako and blue sharks, respectively, overlapped with longline fisheries, but fishing effort within this overlap was also significantly greater (means: mako = 12.2 d ± 9.0 S.D.; blue = 14.0 d ± 9.7 S.D.) compared to other tracked sharks (range, 0.12 – 6.7 d) (Fig. 3a; Extended Data Table 4b; Extended Data Fig. 6). However, exposure risk varied between oceans because although spatial overlap of shortfin mako and blue sharks remained relatively high in the east Pacific (~40%), and at 55.7% for blue shark in Oceania, longline fishing effort was lower there (means: ~1 d in Pacific; 6.6 d in Oceania) (Fig. 3a,b,d; Extended Data Fig. 6).

Among sharks generally considered less commercially valuable, including tiger and bull sharks, we found exposure risk to longlines was high in some but not all regions. Bull sharks used spatially limited areas within southwest Indian Ocean shelf and oceanic island habitats, and in those areas they were at increased risk due to high average overlap (100%) and fishing effort (45.6 d) (Extended Data Table 4d; Extended Data Figure 6j). This greater susceptibility could lead to high localised catches, which, if replicated elsewhere, could explain why bull sharks are one of the ten most commonly traded species in the Hong Kong fin market[26]. In contrast, tiger sharks were exposed to higher than average overlap in the Indian Ocean (87.3%) and Oceania (63%), but fishing effort overlapping this species was lower than average in all oceans (Fig. 3a-d; Extended Data Tables 4d, e).

High risk was evident for internationally protected sharks under CITES (Convention on International Trade in Endangered Species) Appendix II and RFMO regulations. The porbeagle shark (IUCN Red List ‘endangered’ globally) and the white shark (‘vulnerable’

451 globally) have low population sizes compared to historic levels (Supplementary Table 2). In
452 the North Atlantic we found an average 97% overlap of porbeagle space use and higher than
453 average fishing effort (6.7 d) (Fig. 3a), indicating high potential for incidental bycatch
454 mortality. We found white sharks in the highest risk zone in all oceans where it was tracked,
455 with mean spatial overlap with longline fisheries ranging from 55% (east Pacific) to 96%
456 (southwest Indian Ocean) and fishing effort in those areas being between 2.7 d (east Pacific)
457 and 17.0 d (southwest Indian Ocean) (Fig. 3a-d; Extended Data Table 4). Our results showing
458 high fishing overlap and effort for porbeagle and white sharks highlight the need for
459 continued protection – including sufficient scientific observer coverage on vessels to
460 underpin accurate data reporting – in the regions we identify where risk is greatest so that
461 stock rebuilding can continue[27], which for porbeagle is estimated to take a further 30 years[20].

462 The highest levels of exposure risk of sharks to longline fisheries were not constant but
463 varied seasonally as shark and fishing vessel space use shifted in relation to each other (Fig.
464 4; Extended Data Fig. 8). Overall for species with sufficient data (plotted in Fig. 4), the mean
465 monthly overlap of shark space use with longline fishing effort was 40.5% (± 26.9 S.D.;
466 median = 24.2%), similar to the mean annual overlap of 45%. This indicates shark-longline
467 overlap remained relatively high in both space and time. Generally, sharks spent 5–6 months
468 per year in the lowest risk zone and 2–6 months in the highest, with differing patterns of
469 changing exposure to fishing evident across species (Fig. 4). For example, overlap and
470 longline fishing effort for North Atlantic blue and southwest Indian Ocean white sharks both
471 remained relatively high (~60% overlap, ~40 d effort), but with highest risk occurring at
472 discrete times in the year (Extended Data Fig. 9). For Indian Ocean white sharks, this pattern
473 arises from long-range seasonal movements (Feb, Jun/Jul, Oct) into annually persistent areas
474 of high longline fishing effort (>60% overlap, >40 d effort) (Extended Data Fig. 9d). For blue
475 sharks, the discrete pattern appears driven by sharks and longline vessels co-occurring

maximally in boreal winter and summer, with lower exposure risk occurring in boreal spring and autumn as sharks migrate north before returning south[5]. Longline fisheries also made this seasonal south-north-south movement, but lagging behind movements of blue sharks, thus lower overlap and effort during those times (Extended Data Fig. 9a). Similarly, annual risk patterns of east Pacific white and Australian tiger sharks were driven by migratory behaviour, with highest risk (~20% overlap, ~10 d effort) occurring for three consecutive months in boreal (white) and austral (tiger) spring as sharks arrive in areas with higher longline fishing effort (Extended Data Fig. 9c,e). In contrast, shortfin mako sharks in the North Atlantic were exposed to high overlap (>55%) and effort (>32 d) continually through the boreal summer and autumn (Jun–Nov), principally due to occupation of a space use hotspot located where the Gulf Stream and Labrador Current converge that results in persistent high overlap with high longline fishing effort (Fig. 4b; Extended Data Fig. 9b). Shortfin mako and vessel tracking indicates that fishery-induced mortality within this hotspot is therefore likely to be high. This was confirmed by the high return rate of satellite tags (19.3%) attached to Atlantic shortfin makos (n = 119 tags; tracking duration: mean ± SD = 161.5 d ± 156.9; median = 109 d) that were returned to us after sharks were captured by Atlantic longline fishing vessels. To our knowledge, this is the highest species-specific return rate yet recorded in an ocean scale, as opposed to regional scale, study[7,8] (Fig. 2c; Extended Data Table 5; Supplementary Results and Discussion 2.4).

High fishing effort focused on extensive shark hotspots of commercially valuable species raises particular concern. There is limited high seas management for commercial species, including blue and shortfin mako sharks[5,20]. The results from AIS indicate a high probability of overexploitation of commercial species as high seas space use hotspots are exposed to high fisheries overlap across their ranges for significant periods of a year (Extended Data Figs. 6,

9). Overall, this pattern suggests a future with limited spatial refuge from industrial longline fishing effort that is currently centred on ecologically important shark hotspots.

The patterns of high overlap and fishing effort observed for sharks suggest different mechanisms driving shark fishing hotspots. The high overlap and fishing effort observed in commercially important shark hotspots, together with high catches (landings), support the explanation that fishers track sharks. For example, North Atlantic blue and shortfin mako sharks are known target species of Chinese, Spanish and Portuguese longlining fleets[5,14,17] (Extended Data Table 2). However, this is not necessarily the case for all global hotspots. Internationally protected species such as the white shark was subject to high overlap and effort in the North Atlantic, southwest Indian, and northeast and southwest Pacific oceans despite no target fisheries. This indicates that high overlap is due to white sharks co-occurring in habitats of target fish species (e.g. tunas) that fishers track.

Our results show that globally important habitat areas for threatened pelagic sharks overlap significantly with industrial fishing activity in both space and time. Given the high fishing effort in hotspots of many species for significant portions of the year, and the very few tracked hotspots free from exploitation, our study reveals exposure risk of sharks to fisheries in the high seas is spatially extensive – stretching across entire ocean-scale population ranges for some species. The distribution maps reported here are, therefore, a first but essential underpinning for a conservation blueprint for pelagic sharks in this high seas habitat. Our study highlights the scale of fishing overlap with shark hotspots and argues for more effective and timely monitoring, reporting and management of pelagic sharks as a result. To enhance the recovery of vulnerable species, one solution is designation of large–scale MPAs[28] around ecologically important space use hotspots of pelagic sharks[24], notwithstanding the need for more complete reporting of catch data to support stricter conventional management by catch

prohibitions or quotas[5,18]. This study outlines shark hotspot locations where fishing effort is currently relatively low, which is where shark conservation could be maximized, while minimizing impact on fishing activity not directed at sharks. Although the legal framework remains challenging to develop a legally binding treaty for managing high seas fauna[22], burgeoning technology for global surveillance and enforcement now offers valuable additional options for a step change in ocean management[6].

Satellite monitoring of ocean-scale movements by marine megafauna[1,5,13,29], oceanographic features (eddies, fronts)[6,24] and global fishing vessel distributions[21] could provide signals of shifting space use by megafauna due to environmental changes that, in turn, could inform designation of new temporary time-area closures to industrial fishing[6] and tracking of fishers' displacement activities[22]. The potential of AIS as a global fisheries and conservation management tool suggests that, given the remoteness and vast extent of the high seas, if we are to reverse the observed declines and so rebuild populations of iconic ocean predators[3] such as pelagic sharks[14], technology-led conservation measures – conservation technology – will be crucial in addition to conventional management methods[5,18-20]. Conservation technology could evolve in the future toward incorporation of adaptive management strategies that are actionable in real time. The rapid development of autonomous vehicles has created a need to develop machine-learning real-time assessments of risks[30], developments that can be readily transposed to assess risks in the overlap between fishing vessels and sharks across the global ocean.

1. Hays, G.C. *et al.* Key questions in marine megafauna movement ecology. *Trends Ecol. Evol.* **31**, 463-475 (2016).

2. Lewison, R.L. *et al*. Global patterns of marine mammal, seabird, and sea turtle bycatch reveal taxa-specific and cumulative megafauna hotspots. *Proc. Natl. Acad. Sci. USA* **111**, 5271-5276 (2014).

3. McCauley, D.J., Pinsky, M.L., Palumbi, S.R., Estes, J.A. Joyce, F.H., Warner, R.R. Marine defaunation: Animal loss in the global ocean. *Science* **347**, 1255641 (2015).

4. Worm, B., Sandow, M., Oschlies, A., Lotze, H., Myers, R.A. Global patterns of predator diversity in the open oceans. *Science* **309**, 1365-1369 (2005).

5. Queiroz, N. *et al*. Ocean-wide tracking of pelagic sharks reveals extent of overlap with longline fishing hotspots. *Proc. Natl. Acad. Sci. USA* **113**, 1582-1587 (2016).

6. Scales, K.L. *et al*. Fisheries bycatch risk to marine megafauna is intensified in Lagrangian coherent structures. *Proc. Natl. Acad. Sci. USA*, doi:10.1073/pnas.1801270115 (2018).

7. Kohler, N.E., Turner, P.A. Shark tagging: a review of conventional methods and studies. *Environ. Biol. Fish.* **60**, 191-223 (2001).

8. Byrne, M.E. *et al.* Satellite telemetry reveals higher fishing mortality rates than previously estimated, suggesting overfishing of an apex marine predator. *Proc. R. Soc. B* **284**, 20170658 (2017).

9. O'Connor, S., Ono, R., Clarkson, C. Pelagic fishing at 42,000 years before the present and the maritime skills of modern humans. *Science* **334**, 1117-1121 (2011).

10. Tickler, D., Meeuwig, J.J., Palomares, M.-L., Pauly, D., Zeller, D. Far from home: Distance patterns of global fishing fleets. *Sci. Adv.* **4**, eaar3279 (2018).

11. Lea, J.S.E. *et al*. Repeated, long-distance migrations by a philopatric predator targeting highly contrasting ecosystems. *Sci. Rep.* **5**, 11202 (2015).

12. Guzman, H.M., Comez, C.G., Hearn, A., Eckert, S.A. Longest recorded trans-Pacific migration of a whale shark. *Mar. Biodivers. Rec.* **11**, 8, https://doi.org/10.1186/s41200-018-0143-4 (2018).

13. Block, B.A. *et al.* Tracking apex marine predator movements in a dynamic ocean. *Nature* **475**, 86-90 (2011).

14. Worm, B. *et al*. Global catches, exploitation rates, and rebuilding options for sharks. *Mar. Policy* **40**, 194-204 (2013).

15. Baum, J.K. *et al*. Collapse and conservation of shark populations in the North-west Atlantic. *Science* **299**, 389-392 (2003).

16. Ferretti, F., Worm, B., Britten, G.L., Heithaus, M.R., Lotze, H.K. Patterns and ecosystem consequences of shark declines in the ocean. *Ecol. Lett.* **13**, 1055–1071 (2010).

17. Oliver, S., Braccini, M., Newman, S.J., Harvey, E.S. Global patterns in the bycatch of sharks and rays. *Mar. Policy* **54**, 86-97 (2015).

18. Campana, S.E. Transboundary movements, unmonitored fishing mortality, and ineffective international fisheries management pose risks for pelagic sharks in the Northwest Atlantic. *Can. J. Fish. Aquat. Sci.* **73**, 1599-1607 (2016).

19. International Commission for the Conservation of Atlantic Tunas (ICCAT). Report of the 2017 ICCAT Shortfin Mako Assessment Meeting (Madrid, Spain, 2017); (<https://www.iccat.int/Documents/Meetings/Docs/2017_SMA_ASS_REP_ENG.pdf>)

20. International Commission for the Conservation of Atlantic Tunas (2017) Report of the Standing Committee on Research and Statistics (SCRS), Doc. No. PLE 104/2017. (<https://www.iccat.int/Documents/Meetings/Docs/2017_SCRS_REP_ENG.pdf>)

591 21. Kroodsma, D.A. *et al.* Tracking the global footprint of fisheries. *Science* **359**, 904-908
592 (2018). See also Response to Comment; *Science* **361**, eaat7789 (2018).

593 22. McCauley, D.J. *et al*. Marine governance: Ending hide and seek at sea. *Science* **351**,
594 1148-1150 (2016).

595 23. Shepperson, J.L., Hintzen, N.T., Szostek, C.L., Bell, E., Murray, L.G., Kaiser, M.J. A
596 comparison of VMS and AIS data: the effect of data coverage and vessel position
597 recording frequency on estimates of fishing footprints. *ICES J. Mar. Sci.* **75**, 988-998
598 (2018).

599 24. Scales, K.L., Miller, P.I., Hawkes, L.A., Ingram, S.N., Sims, D.W., Votier, S.C. On the
600 front line: frontal zones as priority at-sea conservation areas for mobile marine
601 vertebrates. *J. Appl. Ecol.* **51**, 1575-1583 (2014).

602 25. Howey-Jordan, L.A. *et al*. Complex movements, philopatry and expanded depth range of
603 a severely threatened pelagic shark, the oceanic whitetip (*Carcharhinus longimanus*) in
604 the western North Atlantic. *PLoS One* **8**, e56588 (2013).

605 26. Fields, A.T. *et al*. Species composition of the international shark fin trade assessed
606 through a retail-market survey in Hong Kong. *Conserv. Biol.* **32**, 376-389 (2018).

607 27. Curtis, T.A. *et al*. Seasonal distribution and historic trends in abundance of white sharks,
608 *Carcharodon carcharias*, in the Western North Atlantic Ocean. *PLoS One* **9**, e99240
609 (2014).

610 28. O'Leary, B.C. *et al*. Addressing criticisms of large-scale marine protected areas.
611 *BioScience* **68**, 359-370 (2018).

612 29. Sequeira, A.M.M. *et al*. Convergence of marine megafauna movement patterns in coastal
613 and open oceans. *Proc. Natl Acad. Sci. USA* **115**, 3072-3077 (2018).

614 30. Lefèvre, S., Dizan V. & Laugier, C. A survey on motion prediction and risk assessment
615 for intelligent vehicles. *ROBOMECH Journal* **1**, 1. https://doi.org/10.1186/s40648-014-
616 0001-z (2014).

617 **Acknowledgements.** We thank all involved with the many aspects of fieldwork and data
618 collection; full details are given in the *Supplementary Information*. Data analysis was funded
619 by the Marine Biological Association (MBA) and the UK Natural Environment Research
620 Council (NERC) (NE/R00997X/1) (to D.W.S.), with additional research support from the
621 Save Our Seas Foundation and the NERC Oceans 2025 Strategic Research Programme in
622 which D.W.S. was a principal investigator. D.W.S. was supported by an MBA Senior
623 Research Fellowship, N.Q. by European Regional Development Fund (FEDER) via the
624 Programa Operacional Competitividade e Internacionalização (COMPETE), National Funds
625 via Fundação para a Ciência e a Tecnologia (FCT) under PTDC/MAR/100345/2008 and
626 COMPETE FCOMP-01-0124-FEDER-010580 (to N.Q. and D.W.S.), Norte Portugal
627 Regional Operational Programme (NORTE 2020) under the PORTUGAL 2020 Partnership
628 Agreement through the European Regional Development Fund (ERDF) under project
629 MarInfo (NORTE-01-0145-FEDER-000031), an FCT Investigator Fellowship IF/01611/2013
630 (N.Q.), FCT Doctoral Fellowship PD/BD/52603/2014 (M.V.), and A.M.M.S. was supported
631 by ARC grant DE170100841 and operational funds from the Australian Institute for Marine
632 Science (AIMS). The Tagging of Pacific Predators programme and Global Fishing Watch are
633 thanked for making their data freely available. We thank Marc Dando for creating the shark
634 images. This research contributes to the Global Shark Movement Project (GSMP) and the
635 Marine Megafauna Movement Analytical Program.

Author Contributions. GSMP was coordinated by D.W.S. N.Q. and D.W.S. conceived the study, N.Q., N.E. Humphries and D.W.S. designed the study, and all authors contributed to animal tagging, fieldwork, data collection and/or contribution of tools; full details given in *Supplementary Information*. N.Q., N.E. Humphries, A.C., M.V., I.C., A.M.M.S., L.L.S., S.J.S. and D.W.S. analysed collated data. D.W.S. drafted the paper with contributions from N.Q., N.E. Humphries and A.M.M.S. All authors contributed to subsequent drafts.

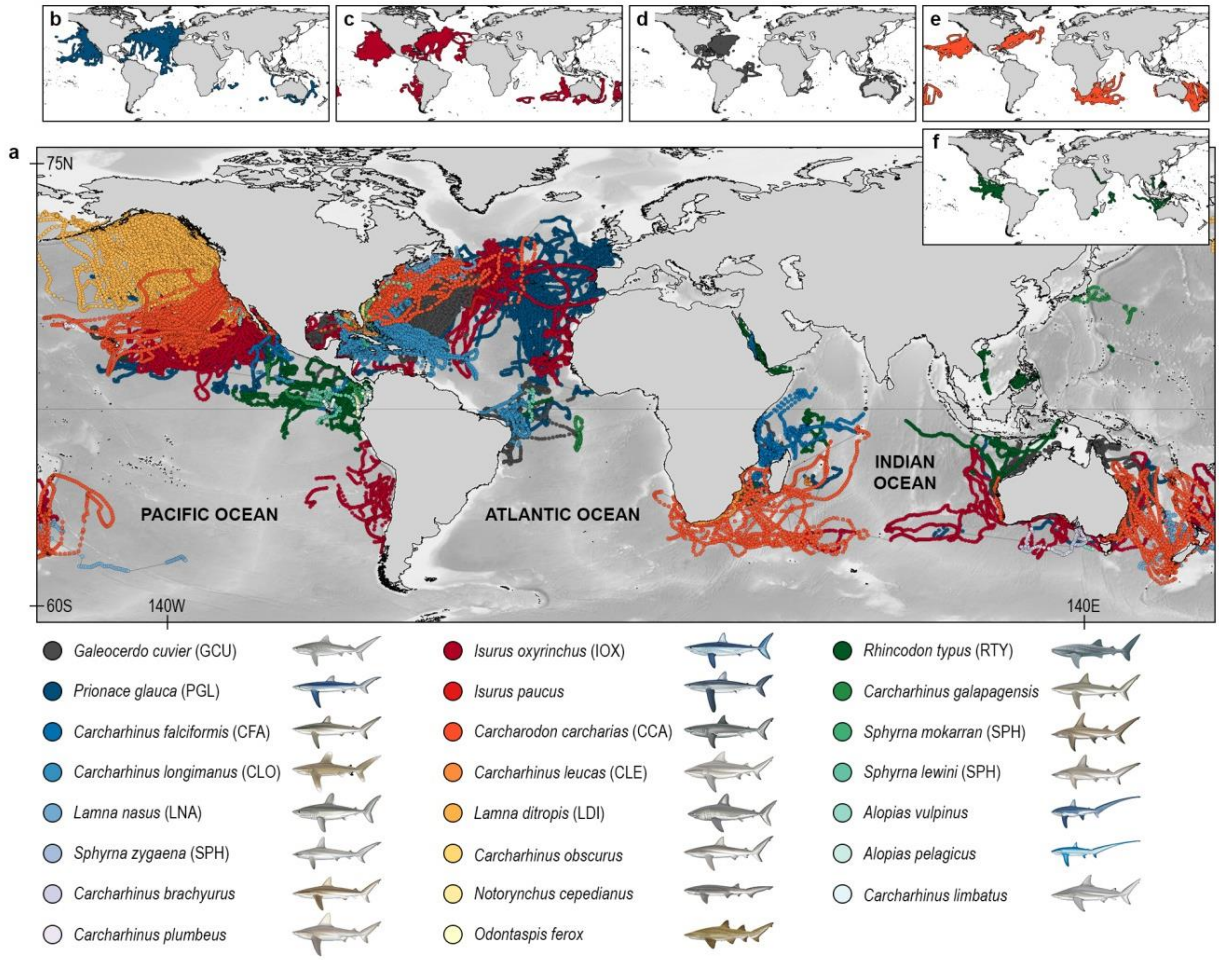

643

644

645 **Fig. 1. Movements of oceanic and neritic pelagic sharks.** (**a**) Daily state-space model
646 locations estimates from raw locations relayed by satellites from transmitters deployed on
647 1,681 sharks from 23 species between 2002–2017. Extent of individual shark species space-
648 use areas are illustrated for blue *Prionace glauca* (**b**), shortfin mako *Isurus oxyrinchus* (**c**),
649 tiger *Galeocerdo cuvier* (**d**), white *Carcharodon carcharias* (**e**) and whale *Rhincodon typus*
650 sharks (**f**). Shark images created by M. Dando.

651

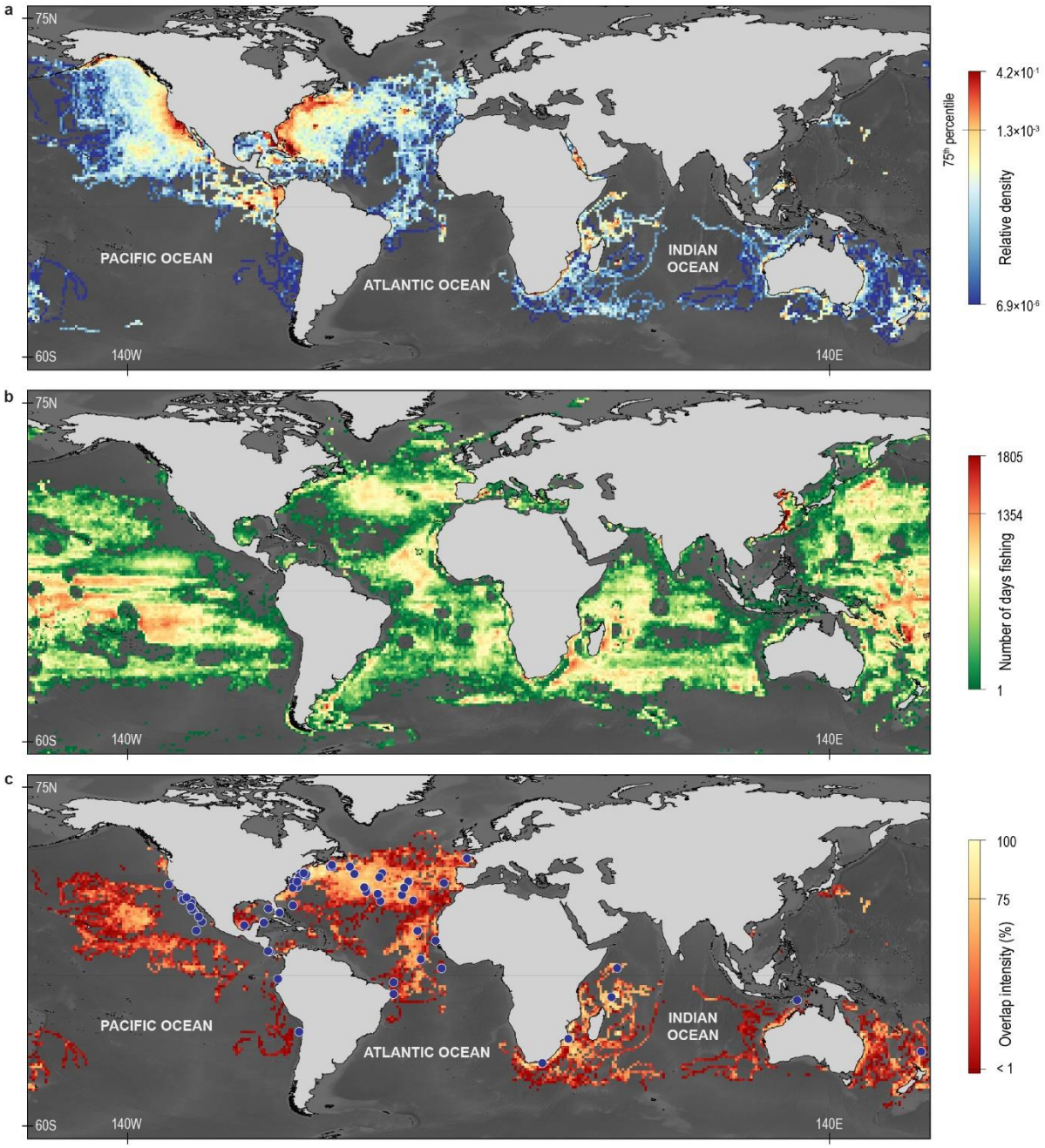

652

653 **Fig. 2. Spatial distributions and overlap intensity of sharks and longline fishing vessels.**
654 (**a**) Distribution of the weighted, normalized location density of ≥75th percentile (relative
655 density) of tracked sharks in 1 × 1° grid cells. (**b**) Mean annual distribution of fishing effort
656 (mean days per grid cell) of AIS tracked longlining vessels in 2012–2016 (see Methods). (**c**)
657 Distribution of the overlap intensity between shark density and longline fishing effort (spatial
658 co-occurrence within 1 × 1° grid cells). Spatial overlap intensity hotspots were defined as 1 ×

659 1° grid cells with ≥75% overlap. Blue circles denote locations where tagged sharks were
660 caught by commercial fishers.

661

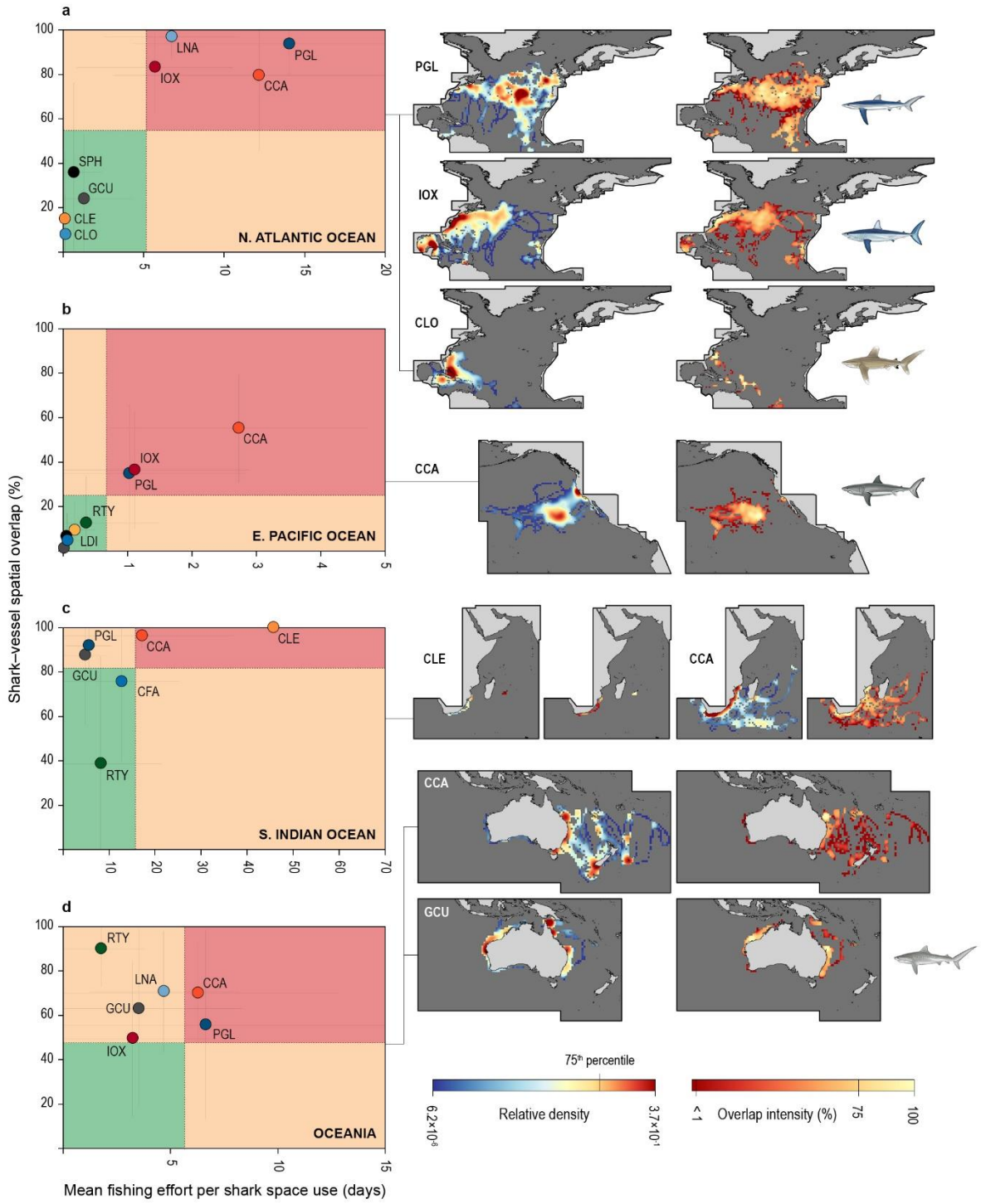

662

663 **Fig. 3. Estimated exposure risk of sharks to capture by longline fishing activity.** Plots
664 (left) showing shark-longline vessel spatial overlap against longline fishing effort per shark
665 space use indicate species subject to high overlap and fishing effort (higher than average
666 overlap and effort; higher risk red zone on plot) and those with lower overlap and effort
667 (lower than average overlap and effort; lower risk green zone) for (**a**) North Atlantic, (**b**)

668 eastern Pacific and (**c**) southern Indian oceans, and (**d**) for the Oceania region. Lines
669 separating the coloured zones are fixed at the average values of spatial overlap (*y* axis) and
670 fishing effort per shark space use (*x* axis) for all species combined. For each ocean, relative
671 density distributions of selected shark species (middle map panels) are shown in comparison
672 to where overlap intensity hotspots of shark-longline vessels occur (map panels on right; see
673 Methods for details). Shark species identification codes (e.g. PGL) used on panels are given
674 in Fig. 1. Error bars denote ± one standard deviation of the mean. Shark images created by M.
675 Dando.
676

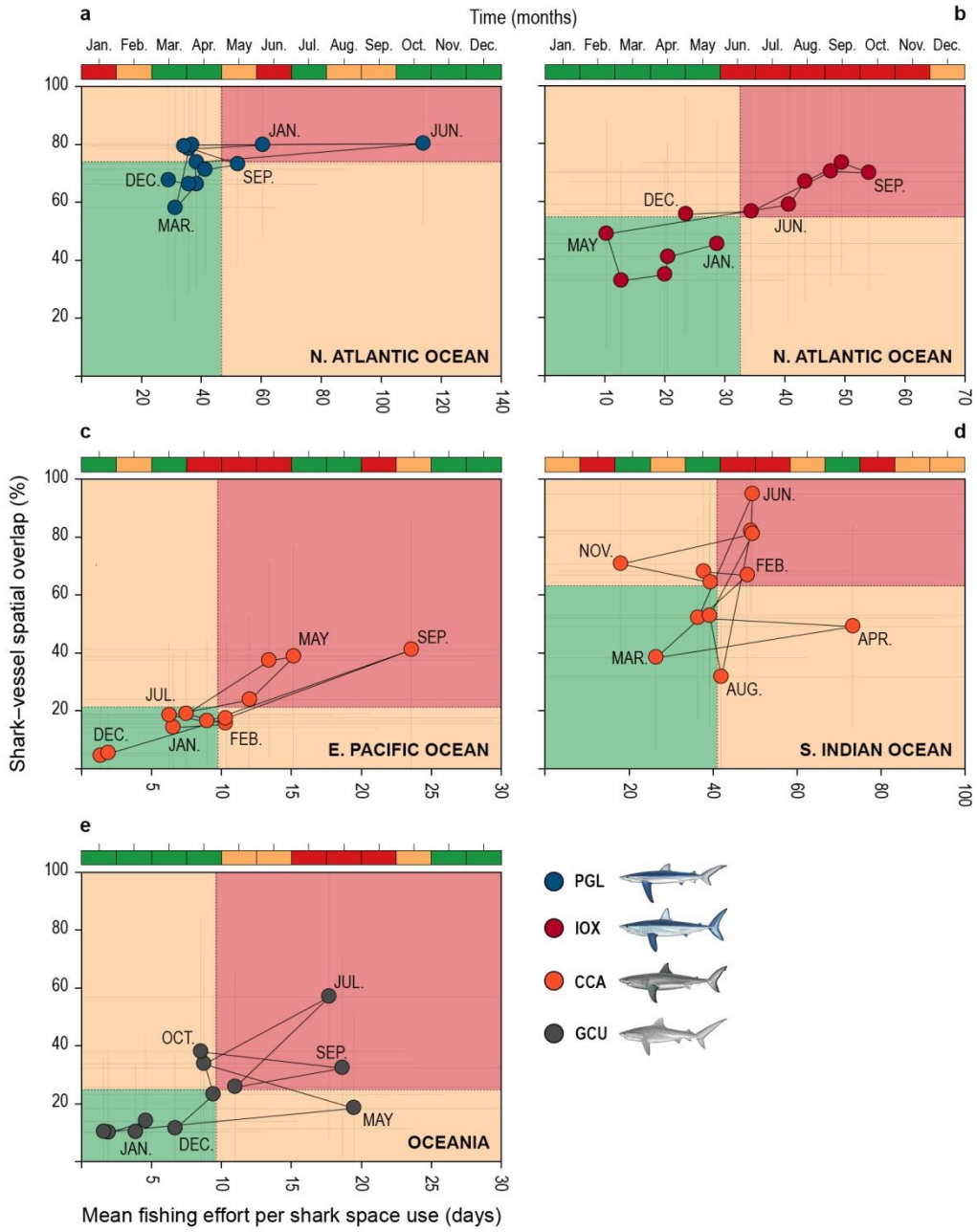

677

678

679 **Fig. 4. Temporal changes in shark exposure risk to longline fishing.** Mean annual shark-
680 longline vessel spatial overlap versus longline fishing effort for the four most data-rich
681 species: (a) blue, (b) shortfin mako, (c, d) white, and (e) tiger sharks. Lines separating the
682 coloured zones are fixed at the respective species average values of spatial overlap (*y* axis)
683 and fishing effort per shark space use (*x* axis). Horizontal bars denote months in different

684 fishing exposure risk zones (red, highest risk; green, lowest). Error bars denote ± one
685 standard deviation of the mean. Shark images created by M. Dando.

686

687 **Methods**

688 **Study animals and tagging.** Satellite transmitter tags were attached to 1,804 large pelagic
689 sharks at multiple tagging sites in the Atlantic, Indian and Pacific oceans (Extended Data Fig.
690 1). The number of tagged individuals varied among species and ranged from one to 280. Two
691 satellite-transmitter tag types (ARGOS, advanced research and global observation satellite
692 transmitter; and PSAT, pop-off satellite-linked archival transmitter) were used. Sharks were
693 either captured with baited hooks (longlines, rod-and-line angling, or with handlines), in
694 purse seine during commercial fishing operations, or tagged free-swimming in the water.
695 Tags were attached to the first dorsal fin or in the dorsal musculature. All animal handling
696 procedures were approved by institutional ethical review committees and completed by
697 trained personnel. Data were provided by the 37 data owners to the senior author and quality
698 checked prior to archiving in a database. Poor quality data were reported for 123 tags (72
699 ARGOS and 51 PSAT) due to, for example, early tag failure, premature tag pop-off, and/or a
700 high percentage of locations estimated with high spatial error, e.g. raw computed
701 geolocations over land, all of which resulted in poor state-space model fits leading to short or
702 unreliable track reconstructions. Hence, analyses were restricted to the remaining 1,681
703 tracks from 1,066 ARGOS and 615 PSAT tags on sharks from 23 species ranging in duration
704 per species from 20 to 57,037 days with a median of 4.1 years total track time per species
705 (Supplementary Table 3). The number of sharks tracked within each region is given in
706 Supplementary Table 9.

707 **Track processing.** Movements of PSAT-tagged sharks were estimated using either satellite
708 relayed data from each tag or from archival data after the tags were physically recovered.
709 Data were provided as: (i) raw shark positions that were previously reconstructed using
710 software provided by the tag manufacturers (e.g. Wildlife Computers, Redmond, USA;
711 Microwave Telemetry, USA), where daily maximal rate-of-change in light intensity was used

712 to estimate local time of midnight or midday for longitude calculations, and day-length
713 estimation for determining latitude[31,32]; or (ii) filtered positions where a state-space model
714 (SSM) (unscented Kalman filter with sea surface temperature, UKFSST)[33] had been applied
715 to correct the raw geolocation estimates and obtain the most probable track. In the first case,
716 raw positions were corrected using the UKFSST SSM (UKFSST R package) in addition to a
717 bathymetric correction applied to the initial Kalman position estimates (analyzepsat R add-
718 on). A daily time-series of locations was estimated using a continuous-time correlated
719 random walk (CTCRW) Kalman filter[34] (crawl R package). UKFSST geolocations were
720 parameterised with standard deviation (SD) constants (K) which produces the smallest mean
721 deviation from concurrent Argos positions[35]. In the latter case, the CTCRW filter was applied
722 to produce regular time-series.

723 For ARGOS transmitter tags, data were provided as raw ARGOS (Doppler frequency shift)
724 position estimates. Location class (LC) Z data – assigned for a failed attempt at obtaining a
725 position – were discarded from the dataset. The remaining raw position estimates (LC 3, 2, 1,
726 0, A and B) were analysed point-to-point with a 3 m s^{-1} speed filter to remove outlier
727 locations. Subsequently, the CTCRW SSM was applied to each individual track, producing a
728 single position estimate per day. ARGOS positions were parameterised with the K error
729 model parameters for longitude and latitude implemented in the *crawl* R package[34].

730 Shark tracking data from the Tagging of Pacific Predators (TOPP) program were downloaded
731 from the Animal Tracking Network (ATN) hosted by the Integrated Ocean Observing System
732 (<https://ioos.noaa.gov/project/atn/>; downloaded September 2017). Both ARGOS and light-
733 based geolocation data in ATN had already been filtered with a Bayesian based SSM[36].
734 Briefly, the SSM was fitted to each track individually, using the WinBUGS software that
735 conducts Bayesian statistical analyses using Markov chain Monte Carlo (MCMC) sampling[37].
736 For each track, two MCMC chains each of length 10,000 were run and a sample of 2,000

737 from the joint posterior probability distribution was obtained by discarding the first 5,000
738 iterations and retaining every 5th of the remaining iterations. SSM fits were posteriorly
739 inspected for obvious problems (e.g. unrealistic movements[13]). Because two different SSMs
740 were applied to data used in this study, we tested for possible biases in the spatial density
741 analysis (see below) by comparing 1 × 1º density grid maps obtained with both UKFSST and
742 Bayesian-based filtered tracks using a subset of 83 ARGOS-linked tracks in the North
743 Atlantic (blue shark, n = 27; mako, n = 42; white, n = 3; oceanic whitetip, n = 11).
744 Differences in spatial grid density between the two methods were negligible (Supplementary
745 Fig. 1).

746 **Spatial density analysis.** To obtain unbiased estimates of shark spatial density, gaps between
747 consecutive dates in the raw tracking data were interpolated to one position per day. The
748 frequency of long temporal gaps in a reconstructed track can result in extensive interpolated
749 movements driven by the underlying random walk model rather than a shark's movement
750 pattern[13]. Although the frequency of long temporal gaps (>20 days) in our dataset was low
751 (Supplementary Table 10), nonetheless, any tracks with gaps exceeding 20 d were split into
752 segments prior to interpolation, thus avoiding the inclusion of unrepresentative interpolated
753 location estimates[5]. Similarly, location estimates derived for periods exceeding 20 d were
754 also discarded from TOPP data[13].

755 To account for biases in spatial density associated with (i) variable track lengths and (ii)
756 shorter tracks near the tagging location, a weighting procedure was applied[13] and data were
757 normalised to account for unequal sample sizes across species. Briefly, each daily location
758 estimate was weighted by the inverse number of individuals of a given species with location
759 estimates for the same relative day. Periods with gaps >20 d were not included when
760 weighting the locations. After the 85th percentile of the track length, daily weights were fixed.
761 Under this weighting scheme, individual location estimates closer to the tagging location

762 received a lower weight than later locations because more sharks had locations earlier in their
763 tracks. Also, longer tracks received a higher total weight than shorter tracks because of the
764 higher number of locations received. Therefore, calculated spatial densities were more
765 representative of the actual distributions and less affected by tag loss, failure or a spatial bias
766 towards deployment location. Total weights for each species were normalised to one so that
767 within the study area each species contributed equally to the density patterns. Species with
768 comparatively very low numbers of tracks were grouped and treated as one (these were: *C.*
769 *galapagensis*, *C. limbatus*, *A. vulpinus*, *A. pelagicus*, *O. ferox*, *C. brachyurus*, *C. obscurus*, *N.*
770 *cepedianus* and *C. plumbeus*). Hammerhead (3 species) and mako (2 species) shark species
771 were also clustered and analysed as taxa groups, *Sphyrna* spp. and *Isurus* spp., respectively.
772 Spatial densities (overall averages) were calculated for all species together (Fig. 2a) and per
773 species at a 1 × 1º grid cell resolution (Extended Data Fig. 6).

774 **Fishing vessel geolocation data.** The automatic identification system (AIS) was developed
775 as a vessel safety and anti-collision system with global coverage, rather than to track fishing
776 vessels for fishery management purposes[21-23]. However, its global coverage of locations of
777 many thousands of ships through time enables fishing effort distribution to be analysed[21,22].
778 Here, fishing effort (hours of fishing) data gridded at 0.01° by flag state and gear type were
779 obtained from Global Fishing Watch (GFW) (available at
780 <http://globalfishingwatch.org/datasets-and-code/fishing-effort/>). GFW used raw AIS vessel
781 tracking data obtained from ORBCOMM via their AIS-enabled satellite constellation
782 (<https://www.orbcomm.com/eu/networks/satellite-ais>) to calculate fishing effort and derive
783 the gridded data, described in detail in Kroodsma *et al.*[21]. Briefly, GFW uses two neural
784 network algorithms to categorize different types of fishing gear, e.g. drifting longlines, purse
785 seines, in addition to estimating the spatio-temporally resolved locations where fishing gears
786 were most likely deployed by individual vessels[21,38]. We used the GFW gridded fishing effort

787 data in the years 2012 to 2016 for all gear types, and for drifting pelagic longlines and purse
788 seines. For each type, we summed the number of days fishing in a year within each 1 × 1°
789 grid cell and averaged across years. For the seasonal analysis, we summed the number of
790 days fishing in each month within each 1 × 1° grid cell and averaged across years. Global
791 distributions of fishing effort for all gear types, longlines and purse seines were mapped
792 separately and overlaid by shark relative spatial density to determine spatial overlap intensity
793 at the global and ocean scale, and for each species per ocean. AIS data coverage increased
794 from 2012 to 2016 as more satellite AIS receivers were launched and commenced
795 operation[21]. However, the global spatial distribution of longline vessel fishing effort was
796 broadly similar across years (Extended Data Fig. 10) and variation in annual maximum
797 fishing effort displayed no increasing trend over time, indicating our calculated mean annual
798 fishing effort for 2012–2016 did not overestimate spatial overlap or fishing effort but can be
799 considered conservative (Extended Data Fig. 10).

800 **Shark and fishing effort environment modelling.** To model shark and fishing vessel
801 distributions in relation to environmental variables, data were extracted from online databases
802 (Supplementary Fig. 2). The environmental variables were selected based upon their
803 demonstrated importance in affecting shark occurrence and included: (i) sea water
804 temperature (ºC) (abbreviation used in models: sea surface temperature, SST; temperature at
805 100 m, TEM_100) known to influence the presence of many pelagic shark species[5,13]; (ii)
806 maximum thermal gradient (ºC/100 km) (TGR) influences shark spatial density[5], and was
807 calculated here based on the SST data and using maximum gradient maps by calculating
808 where for each pixel a geodetic–distance-corrected maximum thermal gradient was
809 calculated; (iii) sea water salinity (psu) (SAL), an important determinant of habitat use in
810 some sharks[1,38]; (iv) sea surface height above geoid (m) (SSH) that influences shark
811 presence[5] and catches by fisheries[6]; (v) ocean mixed layer depth thickness or thermocline

depth (m) (MLD) that affects pelagic shark foraging behaviour[39]; (vi) mass concentration chlorophyll *a* in sea water (mmol m^{-3}) (CHL) as a proxy for productivity that often characterises preferred habitats of sharks[5,39]; (vii) mole concentration of phytoplankton expressed as carbon in sea water concentration (mmol m^{-3}) (PHY) as a direct measure of productivity; (viii) net primary production of biomass expressed as carbon per unit volume in sea water (g m^{-3}/day) (NPP) quantifying productivity; and (ix) mole concentration of dissolved molecular oxygen in sea water (mmol m^{-3}) (DO) that can strongly influence shark space use[1]. Environmental datasets *i* to *v* were downloaded from Copernicus Marine Environment Monitoring Service (CMEMS) Global Ocean Physics Reanalysis product (goo.gl/E4eXDM; downloaded November 2017) and datasets *vi* to *ix* from CMEMS Global Ocean Biochemistry Hindcast product (goo.gl/5hpBs2; downloaded November 2017). CMEMS data were available for 2002 to 2014 from the surface to 5,500 m as monthly datasets. Using custom-written software overall averages (2002-2014) were calculated at a 1 × 1° grid cell resolution for surface and 100 m depth layers (with the exception of SSH and MLD; Supplementary Fig. 2). Most of these variables and interactions are also considered important for explaining fishing patterns[5,6].

We developed and compared a set of generalised additive models (GAMs) with a gaussian family and an identity link using the log-transformed relative density of sharks (D_{it})[13] as response variable. Because we were interested in understanding the general environmental preferences of sharks, we considered the relative density for all 23 shark species combined without considering random effects per species. All environmental variables were standardised and colinearity checked prior to inclusion in the models. Highly skewed environmental variables were logged before standardisation, this included most predictors at the surface (except for SAL and SSH) and also NPP (for sharks only) and TGR at 100 m (TGR_100). The selection of variables to include in each model was made to avoid inclusion

837 of colinear variables in the same model and to specifically address key hypotheses. All
838 possible combinations of 16 variables were not undertaken because many of them are
839 colinear and could not be included in the same model. Rather, we focused on testing
840 ecologically relevant hypotheses. A description of the general hypothesis tested with each
841 model included in the model set is given in Supplementary Table 7. Including models with a
842 reduced number of variables was also necessary, as some variables were colinear with
843 variables included in other models. Because sharks respond to surface and subsurface thermal
844 gradients which often support higher biological productivity[5,6,13,39], we tested for interactions
845 between MLD and SST, CHL and MLD at 100 m (MLD_100), CHL at 100 m (CHL_100)
846 and TEM at 100 m (TEM_100), MLD and TGR at the surface, MLD and CHL_100,
847 CHL_100 and TEM_100, and between SAL and TEM_100.

848 GAM with a Tweedie distribution and log link function provided the best modelling approach
849 for the fishing effort, as this distribution includes a family of probability distributions
850 including normal, gamma, Poisson and compound Poisson-gamma. We considered two
851 response variables separately: fishing effort of all vessels, and fishing effort of longline
852 vessels only. In our model set we included different combinations of a total of the same 16
853 explanatory environmental variables used for shark density modelling (see previous section;
854 Supplementary Table 7), and also a null (all terms equal to zero), intercept-only model. The
855 dimension basis for all terms was limited to 5 (i.e., $k = 5$) to assist controlling for
856 overfitting[40]. We then used the Akaike's information criterion (AIC)[41] to compare the models
857 in the model set for all sharks and fishing vessels. We assessed the relative strength of
858 evidence for each model using the weights of AIC, and the goodness of fit of each model by
859 calculating the percentage of deviance explained (%DE). All models were implemented in R
860 using the mgcv package[42].

Shark/vessel spatial overlap and effort. The spatial overlap (%) between an individual tracked shark and fishing effort was calculated as the number of days that sharks and fishing effort (days) occurred in the same 1 × 1° grid cells in an average year, as a function of all shark grid cells occupied and standardised for shark track length, and summarised as:

Spatial overlap (%) = (number of days with overlap) / (total number of track days) × 100

A fixed 1 × 1° geographic grid cell (where 1° latitude at the equator = 110.6 km) was chosen because it encompassed the maximum length of fishing gear deployed by a single vessel, i.e. the length of drifting longlines are typically 100 km in total length[5]. We examined the effect of grid cell size[43] on spatial overlap estimates by calculating the overlap of all sharks tracked with ARGOS transmitters (~0.5 – 11 km spatial accuracy[44]) with all fishing vessels, then with longliners separately, at 0.5 × 0.5° and 0.25 × 0.25° grid cell sizes. An estimate of fishing effort that an individual shark was exposed to within the space each occupied was termed fishing effort per shark space use and calculated as:

Individual shark exposure to fishing effort (d) = (total number of fishing days) / (total number of track days)

Spatial overlap and fishing effort were also calculated for each of the most data-rich species per month to assess changes within an average year. To determine the spatial variation in overlap and fishing effort within the space used by sharks for mapping purposes, we calculated the overlap intensity in each 1 × 1° grid cell as the product of shark density (number of daily locations) and the number of fishing days.

To test for differences in exposure risk of sharks to fishing activity between different species within the general fishing areas designated by the Food and Agriculture Organization of the United Nations (FAO) (Supplementary Fig. 3), we undertook statistical analysis of exposure risk calculated for each shark as the product of the mean spatial overlap and mean fishing

885 effort. Since data were not normal (Shapiro-Wilk normality test, $p < 0.05$), a Kruskal–Wallis
886 (KW) test was performed (with pairwise Wilcoxon rank sum tests as a post-hoc test).
887 Because of differences in the number of tagged individuals per species, groups of >25 sharks
888 per species were randomly selected and the KW test performed. This procedure was repeated
889 1,000 times and the percentage of times that significant differences were observed were
890 recorded. Species with fewer than 25 individuals tracked were removed from the analysis.
891 Given the relatively low number of sharks tracked in the southwest Indian Ocean and
892 Oceania regions (Supplementary Table 10), statistical tests were restricted to the North
893 Atlantic and eastern Pacific regions. In the Atlantic selected species were: *P. glauca* (*n* =
894 152), *Isurus* spp. (*n* = 120), *G. cuvier* (*n* = 131), *C. carcharias* (*n* = 26), *C. longimanus* (*n* =
895 99), *L. nasus* (*n* = 46), *C. leucas* (*n* = 38) and Sphyrna spp. (*n* = 40); Pacific, species were: *P.*
896 *glauca* (*n* = 112), *I. oxyrinchus* (*n* = 113), *L. ditropis* (*n* = 172), *R. typus* (*n* = 77) and *C.*
897 *carcharias* (*n* = 59).

898 **Shark landings.** Annual pelagic shark landings by species/taxa groups were obtained from
899 the FAO database (<FAO.org/fishery/statistics/global-capture-production/query/en>;
900 downloaded September 2018) and related to fishing effort per shark space use of each
901 species/taxa group. Landings reported for the North Atlantic (northwest, northeast, western
902 central and eastern central Atlantic) between 2012 and 2016 were used in the analysis since it
903 spanned the period that longline fishing effort was monitored (2012–2016). Data were
904 extracted for nine species or taxa groups that are regularly caught by shelf and/or high-seas
905 fisheries in the North Atlantic, the region in which most tags were deployed. The species/taxa
906 groups were: *P. glauca*, *I. oxyrinchus*, *C. longimanus*, *C. leucas*, *C. falciformis*, *L. nasus*, *G.*
907 *cuvier*, *C. carcharias*, and hammerheads (*Sphyrna* spp.) comprising *S. lewini*, *S. mokarran*
908 and *S. zygaena*. Mean annual landings (t) per species/taxa group were calculated and related
909 to AIS longline fishing effort per shark space use.

Additional references

31. Wilson, R.P., Ducamp, J.-J., Rees, W.G., Culik, B.M., Niekamp, K. Estimation of location: global coverage using light intensity. In *Wildlife Telemetry* (eds Priede, I.G., Swift, S.M.), p. 131-134 (Ellis Horwood, Chichester, UK, 1992).

32. Delong, R.L., Stewart, B.S., Hill, R.D. Documenting migrations of northern elephant seals using day length. *Mar. Mamm. Sci.* **8**, 155-159 (1992).

33. Lam, C., Nielsen, A., Sibert, J. Improving light and temperature based geolocation by unscented Kalman filtering. *Fish. Res.* **91**, 15-25 (2008).

34. Johnson, D.S., London, J.M., Lea, M.-A. & Durban, J.W. Continuous-time correlated random walk model for animal telemetry data. *Ecology* **89**, 1208-1215 (2008).

35. Sippel, T., Holdsworth, J., Dennis, T., Montgomery, J. Investigating behaviour and population dynamics of striped marlin (*Kajikia audax*) from the southwest Pacific Ocean with satellite tags. *PLoS One* **6**, e21087 (2011).

36. Jonsen, I.D., Flemming, J.M., Myers, A.E. Robust state-space modeling of animal movement data. *Ecology* **86**, 2874-2880 (2005).

37. Lunn, D. J., Thomas, A., Best, N., Spiegelhalter, D. WinBUGS - a Bayesian modelling framework: 472 concepts, structure, and extensibility. *Statistics Comput.* **10**, 325–337 (2000).

38. Ward-Paige, C.A., Britten, G.L., Bethea, D.M., Carlson, J.K. Characterizing and predicting essential habitat features for juvenile coastal sharks. *Marine Ecology* **36**, 1–13 (2014).

931 39. Queiroz, N., Vila-Pouca, C., Couto, A., Southall, E.J., Mucientes, G., Humphries, N.E.,
932 Sims, D.W. Convergent foraging tactics of marine predators with different feeding
933 strategies across heterogeneous ocean environments. *Front. Mar. Sci.* **4**, 239 (2017).

934 40. Fisher, R., Wilson, S.K., Sin, T.M., Lee, A.C. & Langlois, T.J. A simple function for full-
935 subsets multiple regression in ecology with R. *Ecol. Evol.* **8**, 6104-6113 (2018).

936 41. Burnham, K. P., Anderson, D.R. Multimodel inference: understanding AIC and BIC in
937 model selection. *Sociological Meth. Res.* **33**, 261-304 (2004).

938 42. Wood, S.N. Fast stable restricted maximum likelihood and marginal likelihood estimation
939 of semiparametric generalized linear models. *J. Roy. Statistical Soc.* B **73**, 3-36 (2011).

940 43. Amoroso, R.O., Parma, A.M., Pitcher, C.R., McConnaughey, Jennings, S. Comment on
941 "Tracking the global footprint of fisheries". *Science* **361**, eaat6713 (2018).

942 44. Costa, D.P. *et al*. Accuracy of ARGOS locations of pinnipeds at-sea estimated using
943 Fastloc GPS. *PLoS One* **5**, e8677 (2010).

944

945

946

Extended Data Table 1. Summary of fitted generalised additive models (GAM) relating the log-transformed weighted relative density of all sharks (D_{it}) and the fishing effort of all vessels and of longlines only to environmental variables. Environmental variables included in each model are detailed in Supplementary Table 7. *wAIC* indicates the weight of the Akaike's information criteria for each model in the model set with bold highlighting the highest ranked model. The percentage of deviance explained (%DE) by each model is given and the highest and second highest values for each response variable are highlighted in bold.

Model	***D*$_{it}$**		**Fishing effort (all vessels)**		**Longline fishing effort**	
	wAIC	%DE	*wAIC*	%DE	*wAIC*	%DE
1	**1.000**	**26.25**	**1.000**	**29.88**	**1.000**	**16.12**
2	0.000	20.23	0.000	16.12	0.000	12.90
3	0.000	9.42	0.000	14.52	0.000	14.62
4	0.000	8.21	0.000	9.49	0.000	5.73
5	0.000	5.83	0.000	7.20	0.000	11.14
6	0.000	**21.13**	0.000	**24.89**	0.000	**14.99**
7	0.000	12.01	0.000	17.72	0.000	6.21
8	0.000	0.00	0.000	0.00	0.000	0.00

Extended Data Table 2. The number (**a**) and total hours fished (**b**) by flag state of the 5,565 AIS longline fishing vessels analysed in this study arranged by the largest twenty values (totals for 2012 – 2016). In (a) the number of vessels per flag state is the total number of unique Maritime Mobile Safety Identity (MMSI) codes present in the dataset in 2012 – 2016. In (b), the total longline hours fished is the total during 2012 – 2016.

(**a**)

Flag state	**No. AIS longline vessels**	**% total**
China	2,646	47.55
Taiwan	791	14.21
Japan	460	8.27
Korea	248	4.46
Spain	227	4.08
USA	187	3.36
Portugal	67	1.20
Canada	65	1.17
Vanuatu	63	1.13
Fiji	46	0.83
Australia	43	0.77
India	39	0.70
Russia	35	0.63
South Africa	33	0.59
Seychelles	28	0.50
Argentina	27	0.49
Greece	22	0.40
Italy	22	0.40
New Caledonia	21	0.38
France	20	0.36

973 (**b**)

Flag state	**Total longline hours fished**	**% total**
China	5,227,295	20.81
Taiwan	4,476,896	17.82
Korea	4,292,482	17.09
Japan	3,996,883	15.91
Spain	2,972,677	11.83
Portugal	630,843	2.51
Vanuatu	425,445	1.69
Fiji	284,558	1.13
USA	278,485	1.11
Australia	191,313	0.76
New Caledonia	187,137	0.74
Russia	168,067	0.67
Reunion Islands	164,682	0.66
Chile	164,423	0.65
Argentina	159,235	0.63
South Africa	157,890	0.63
Seychelles	135,016	0.54
France	129,678	0.52
Malaysia	104,742	0.42
Canada	86,943	0.35

974

975

Extended Data Table 3. Effect of different grid cell size on the global mean spatial overlap of sharks and fishing vessels calculated for all ARGOS transmitter tracked sharks (*n* = 1066) and all fishing vessels (including longline), and sharks and all longline vessels separately. ARGOS tracked sharks were used in the analysis because the spatial accuracy of locations was <11 km (see Methods for explanation).

	Grid cell size	**Mean spatial overlap (%)**	**One standard deviation**
Sharks and all fishing vessels (incl. longline)	1 × 1°	81.77	28.48
	0.5 × 0.5°	67.17	35.39
	0.25 × 0.25°	56.47	36.31
Sharks and all longline vessels	1 × 1°	39.21	40.91
	0.5 × 0.5°	30.26	37.63
	0.25 × 0.25°	24.00	33.62

Extended Data Table 4. Calculated mean spatial overlap and fishing effort for ocean regions and species. S.D., ± one standard deviation of the mean; S.E., ± one standard error of the mean. Ocean regions were selected based upon FAO fishing regions (see Supplementary Figure 3). There were 70 individual sharks that did not fall into FAO regions and these were not included in this analysis.

(a) All ocean regions. Calculated spatial overlap and longline fishing effort for the 11 most data-rich species/taxa groups.

Species	**N tags**	**Mean spatial overlap (%)**	**Median**	**S.D.**	**S.E.**	**Mean fishing effort (days)**	**Median**	**S.D.**	**S.E.**
Prionace glauca	280	68.5	90.5	37.3	2.2	8.4	5.4	9.7	0.6
Carcharhinus leucas	41	21.2	0.0	36.5	5.7	3.4	0.0	13.1	2.0
Isurus oxyrinchus	262	57.9	61.3	36.9	2.3	6.4	1.9	8.2	0.5
Carcharhinus longimanus	105	10.9	1.3	20.8	2.0	0.2	0.0	0.4	0.0
Lamna nasus	56	92.1	100.0	17.2	2.3	6.4	5.7	4.1	0.5
Lamna ditropis	172	8.8	2.8	13.1	1.0	0.2	0.0	0.3	0.0
Carcharhinus falciformis	51	52.2	69.5	45.2	6.3	8.0	1.0	11.6	1.6
Sphyrna spp.	66	29.3	10.5	37.7	4.6	0.7	0.0	1.9	0.2
Galeocerdo cuvier	254	40.8	27.3	41.0	2.6	2.0	0.4	3.7	0.2
Rhincodon typus	164	27.7	0.0	39.6	3.1	2.8	0.0	8.0	0.6
Carcharodon carcharias	160	72.2	78.2	26.0	2.1	7.1	3.8	11.2	0.9
Total tags or *Mean*	1611	*43.8*				*4.2*			

(b) North Atlantic. Calculated spatial overlap and longline fishing effort for the 11 most data-rich species/taxa groups.

Species	**N tags**	**Mean spatial overlap (%)**	**Median**	**S.D.**	**S.E.**	**Mean fishing effort (days)**	**Median**	**S.D.**	**S.E.**
Prionace glauca	152	93.7	100.0	14.2	1.2	14.0	11.5	9.7	0.8
Carcharhinus leucas	38	15.0	0.0	29.9	4.9	0.1	0.0	0.2	0.0
Isurus oxyrinchus	120	79.4	99.6	33.8	3.1	12.2	11.3	9.0	0.8
Carcharhinus longimanus	99	8.0	0.5	17.4	1.7	0.1	0.0	0.4	0.0
Lamna nasus	46	96.8	100.0	9.3	1.4	6.7	6.0	4.2	0.6
Lamna ditropis									
Carcharhinus falciformis	1*	100.0	100.0			1.0	1.0		
Sphyrna spp.	40	35.8	15.0	40.1	6.3	0.7	0.1	1.7	0.3
Galeocerdo cuvier	131	23.9	12.7	29.6	2.6	1.3	0.1	2.9	0.3
Rhincodon typus	3	60.2	56.3	25.6	14.8	6.2	0.9	9.7	5.6
Carcharodon carcharias	26	83.3	90.9	21.3	4.2	5.7	4.5	4.8	0.9
Total tags or *Mean*	656	*55.1*				*4.8*			

*The single tag was not included in the mean overlap or effort values shown.

(c) East Pacific. Calculated spatial overlap and longline fishing effort for the 11 most data-rich species/taxa groups.

Species	**N tags**	**Mean spatial overlap (%)**	**Median**	**S.D.**	**S.E.**	**Mean fishing effort (days)**	**Median**	**S.D.**	**S.E.**
Prionace glauca	112	34.5	24.7	31.3	3.0	1.0	0.3	1.8	0.2
Carcharhinus leucas									
Isurus oxyrinchus	113	36.1	34.3	26.4	2.5	1.1	0.8	1.8	0.2
Carcharhinus longimanus	2	62.1	62.1	3.0	2.1	0.4	0.4	0.2	0.1
Lamna nasus									
Lamna ditropis	172	8.8	2.8	13.1	1.0	0.2	0.0	0.3	0.0
Carcharhinus falciformis	17	4.2	0.0	11.9	2.9	0.1	0.0	0.2	0.1
Sphyrna spp.	21	6.0	0.0	10.7	2.3	0.0	0.0	0.1	0.0
Galeocerdo cuvier	12	0.6	0.0	1.6	0.5	0.0	0.0	0.0	0.0
Rhincodon typus	77	12.2	0.0	20.9	2.4	0.4	0.0	1.1	0.1
Carcharodon carcharias	59	55.0	58.2	24.4	3.2	2.7	2.8	2.0	0.3
Total tags or *Mean*	585	*24.4*				*0.7*			

(d) Indian Ocean. Calculated spatial overlap and longline fishing effort for the 11 most data-rich species/taxa groups.

Species	**N tags**	**Mean spatial overlap (%)**	**Median**	**S.D.**	**S.E.**	**Mean fishing effort (days)**	**Median**	**S.D.**	**S.E.**
Prionace glauca	5	91.9	100.0	11.4	5.1	5.4	4.4	4.9	2.2
Carcharhinus leucas	3	100.0	100.0	0.0	0.0	45.6	47.2	23.6	13.6
Isurus oxyrinchus									
Carcharhinus longimanus									
Lamna nasus									
Lamna ditropis									
Carcharhinus falciformis	33	75.5	93.6	35.7	6.2	12.4	8.4	12.5	2.2
Sphyrna spp.									
Galeocerdo cuvier	26	87.3	100.0	31.0	6.1	4.7	4.0	4.8	0.9
Rhincodon typus	48	38.7	0.0	48.2	7.0	8.0	0.0	13.1	1.9
Carcharodon carcharias	34	96.3	98.6	5.2	0.9	17.0	8.3	19.8	3.4
Total tags or *Mean*	149	*81.6*				*15.5*			

(e) Oceania. Calculated spatial overlap and longline fishing effort for the 11 most data-rich species/taxa groups.

Species	**N tags**	**Mean spatial overlap (%)**	**Median**	**S.D.**	**S.E.**	**Mean fishing effort (days)**	**Median**	**S.D.**	**S.E.**
Prionace glauca	11	55.7	71.4	42.3	12.8	6.6	1.6	9.3	2.8
Carcharhinus leucas									
Isurus oxyrinchus	15	49.5	40.3	34.8	9.0	3.2	1.0	3.6	0.9
Carcharhinus longimanus									
Lamna nasus	10	70.5	78.0	27.2	8.6	4.7	4.0	3.4	1.1
Lamna ditropis									
Carcharhinus falciformis									
Sphyrna spp.									
Galeocerdo cuvier	58	62.8	89.4	44.2	5.8	3.5	1.3	4.8	0.6
Rhincodon typus	16	89.8	100.0	16.6	4.1	1.7	0.6	2.0	0.5
Carcharodon carcharias	41	70.0	76.1	22.3	3.5	6.3	3.9	6.5	1.0
Total tags or *Mean*	151	*66.4*				*4.3*			

Ex**tended Data Table 5.** Tag recapture data for the most data-rich species studied.

	Global			**North Atlantic**			**Eastern Pacific**			**Indian Ocean**			**Oceania**		
Shark species	**Total tagged**	**No. recaught**	**%**	**Total tagged**	**No. recaught**	**%**	**Total tagged**	**No. recaught**	**%**	**Total tagged**	**No. recaught**	**%**	**Total tagged**	**No. recaught**	**%**
Silky	51	4	7.84	1	0	0	17	2	11.76	28	2	7.14			
Tiger	254	7	2.76	131	5	3.82	12	0	0	26	0	0	58	0	0
Blue	280	17	6.07	152	12	7.89	112	5	4.46	5	0	0	11	0	0
White	160	2	1.25	26	0	0	59	0	0	34	2	5.88	41	0	0
Mako	261	30	11.49	119	23	19.3	113	5	4.42				15	1	6.67
Salmon	172	1	0.58				172	1	0.58						
Porbeagle	56	3	5.36	46	3	6.52							10	0	0
Whale	134	1	0.61	3	0	0	77	0	0	18	0	0	16	1	6.25
	1398	*65*	*4.65*	*478*	*43*	*9.00*	*562*	*13*	*2.31*	*111*	*4*	*3.60*	*151*	*2*	*1.32*

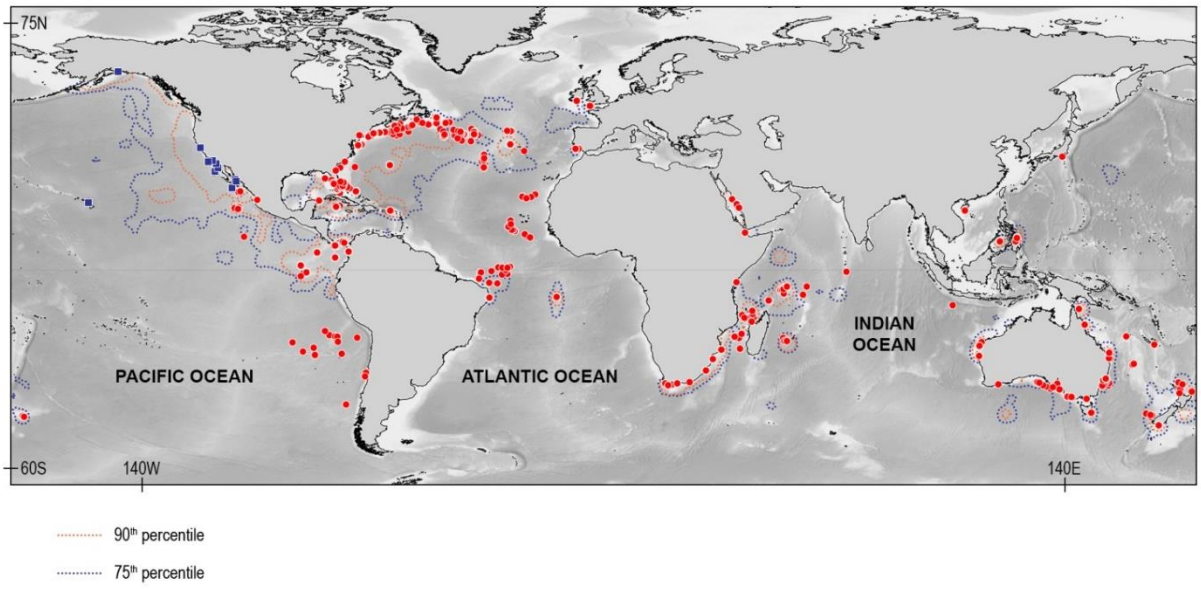

Extended Data Fig. 1. The location of shark tag deployment sites in relation to shark space use hotspots. Red circles denote the locations where satellite transmitters were attached and sharks released, and blue squares in the eastern Pacific denote annual median deployment locations of tags by the Tagging of Pacific Predators (TOPP) program (ref. 13). Shark space use hotspots are shown as the 75th (blue dotted lines) and 90th percentiles (red dotted lines) of the relative density of estimated shark positions within 1 × 1° grid cells given in Fig. 2a.

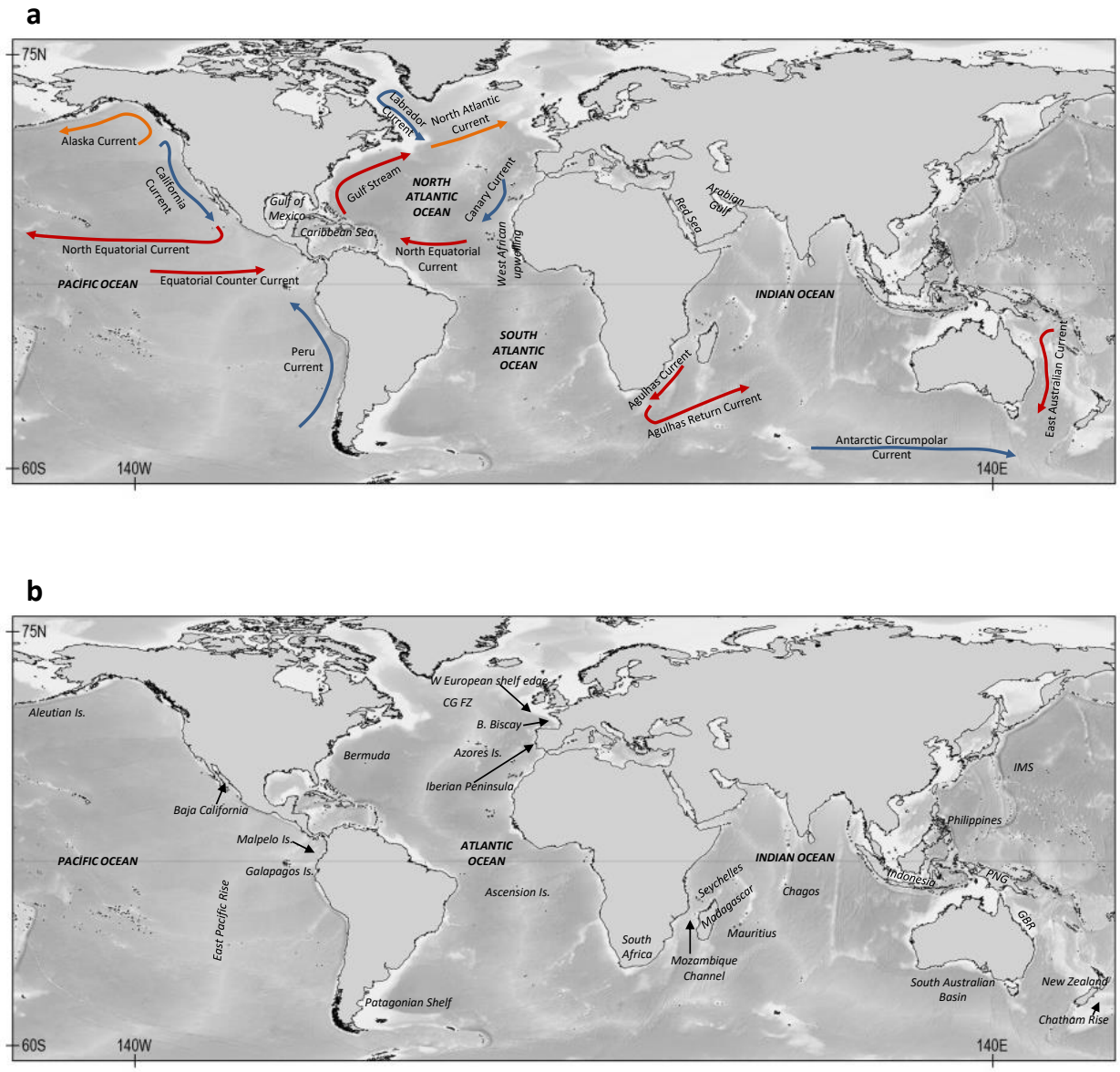

Extended Data Fig. 2. Schematic maps of oceanographic and physical features. Major ocean currents (**a**) and physical features (**b**) referred to in this paper. Coloured arrows in **a** denote thermal regime of currents, with warmer colours indicating greater water temperature. Abbreviations in **b** denote: CGFZ, Charlie Gibbs Fracture Zone; GBR, Great Barrier Reef; PNG, Papua New Guinea; IMS, Isakov and Makarov Seamounts.

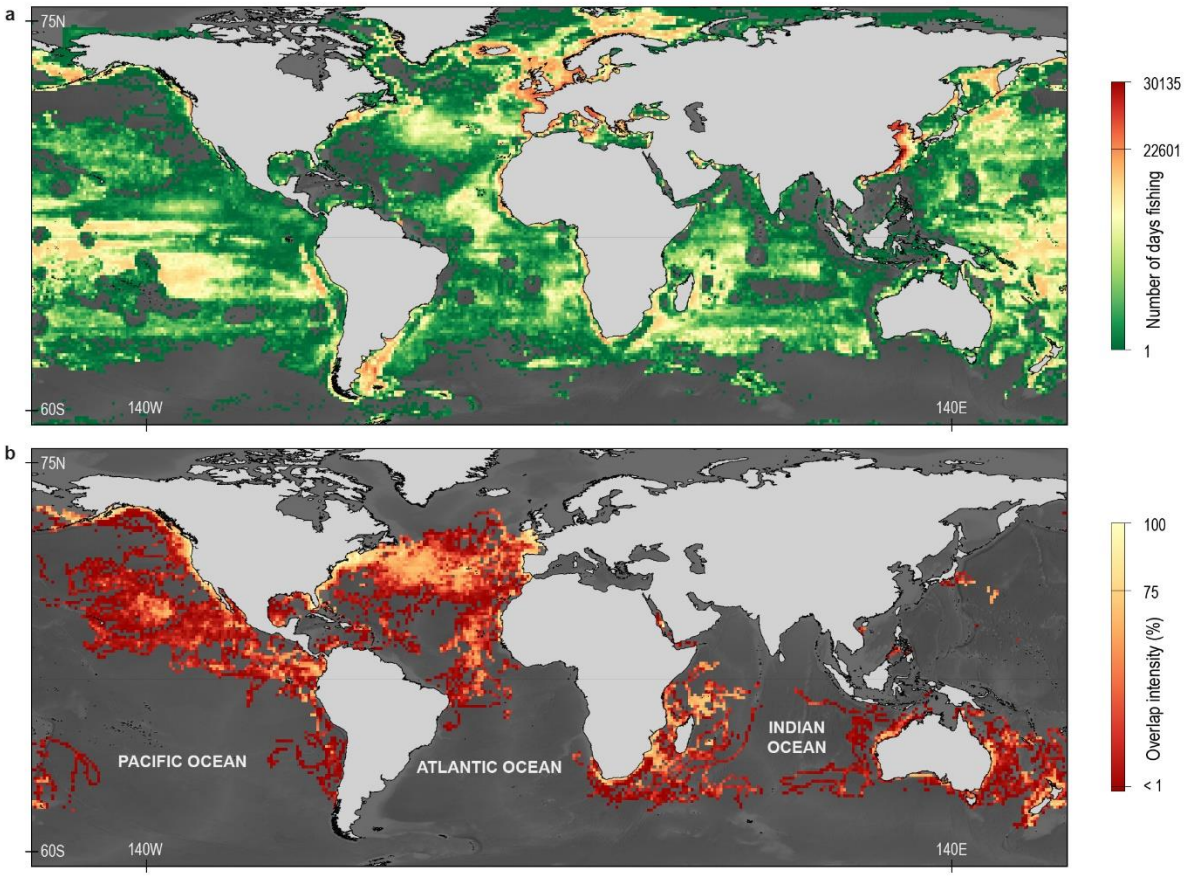

Extended Data Fig. 3. Spatial distribution of fishing vessels and overlap intensity with sharks. (**a**) Distribution of 83,628 AIS tracked fishing vessels' effort (mean annual days spent per grid cell) between 2012 and 2016 (see Methods). (**b**) Distribution of the overlap intensity between shark density and fishing effort (spatial co-occurrence within 1 × 1° grid cells). Spatial overlap intensity hotspots were defined as 1 × 1° grid cells with ≥75% overlap. Note the similar overlap intensity pattern of sharks and all mapped AIS fishing vessels as that determined for sharks and longline vessels in Fig. 2c.

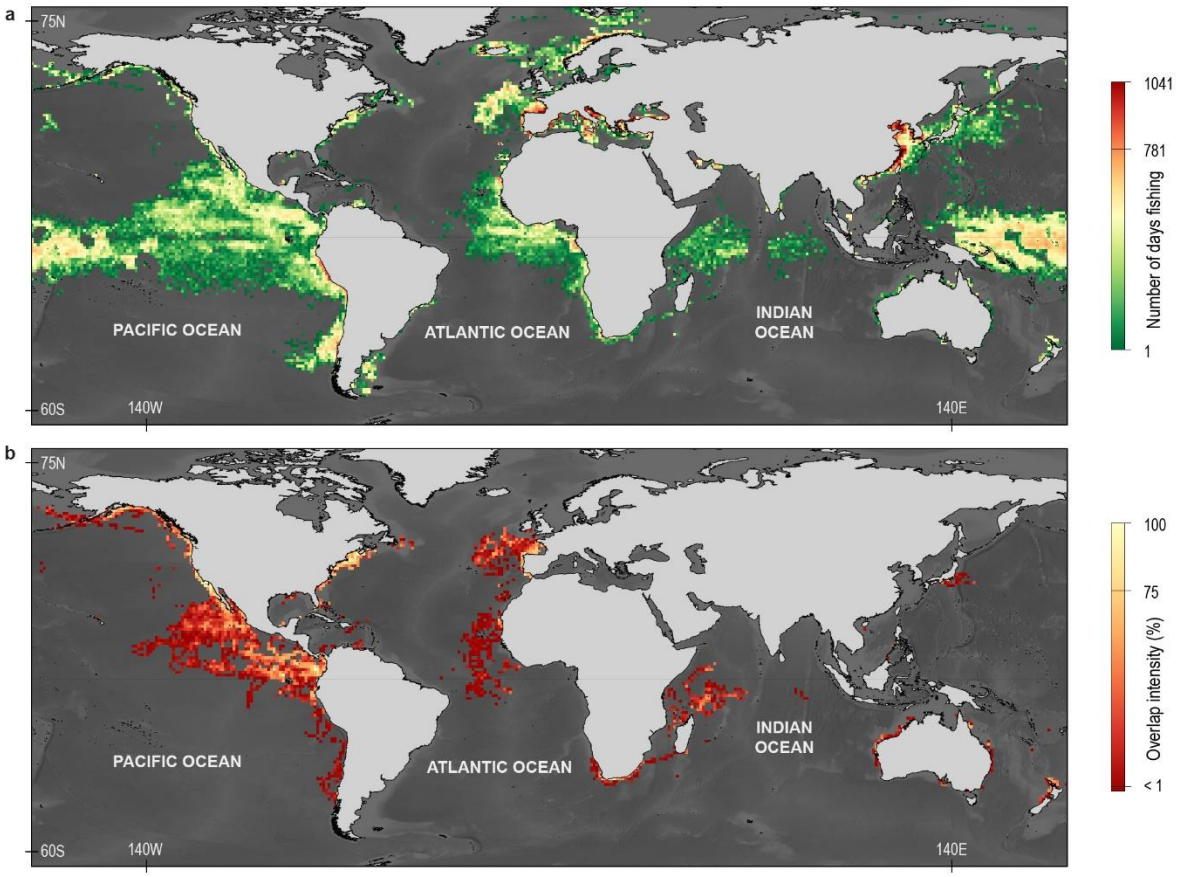

Extended Data Fig. 4. Spatial distribution of purse seine fishing vessels and overlap intensity with sharks. (**a**) Distribution of 6,941 AIS purse seine vessels' fishing effort (mean annual days spent per grid cell) between 2012 and 2016 (see Methods). (**b**) Distribution of the overlap intensity between shark density and fishing effort (spatial co-occurrence within 1 × 1° grid cells). Spatial overlap intensity hotspots were defined as 1 × 1° grid cells with ≥75% overlap.

		MLD_0m	TGR_0m	Interaction	SSH_0m	CHL-a_0m	SAL_100m
Shark spatial density	MODEL 1	*** 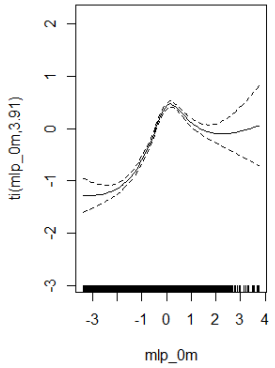	*** 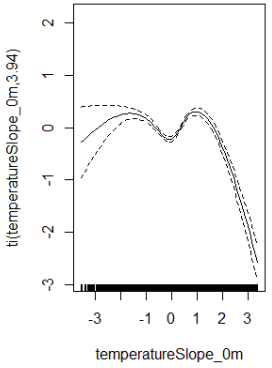	*** 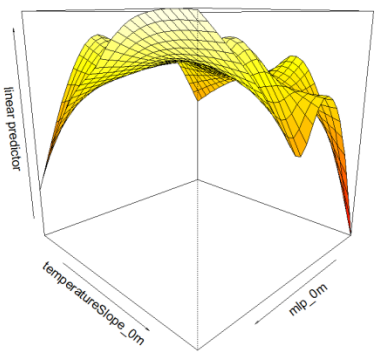	*** 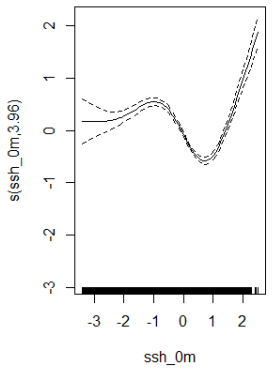	*** 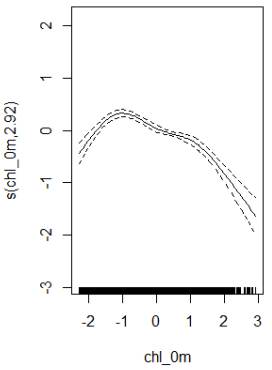	*** 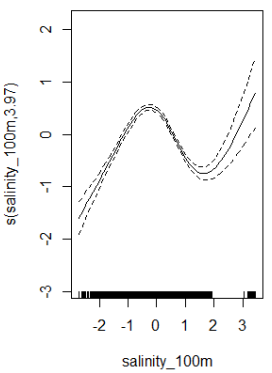
Fishing Effort (all vessels)	MODEL 1	*** 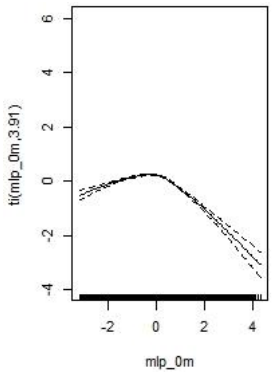	*** 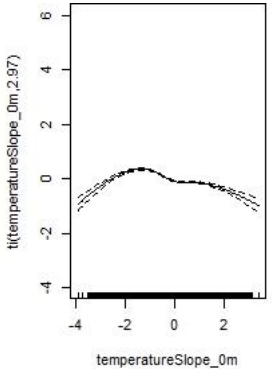	*** 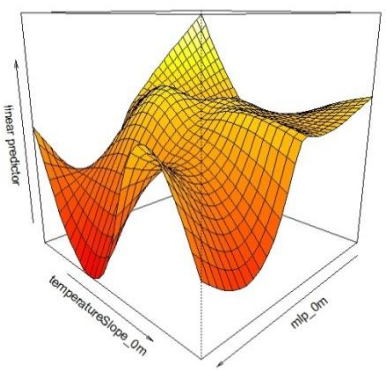	*** 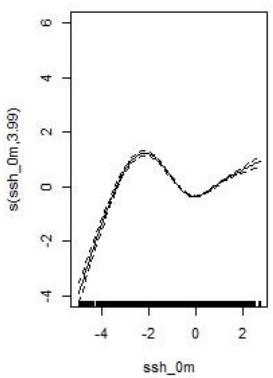	*** 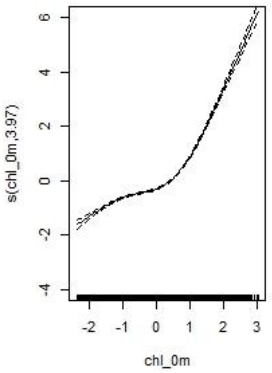	*** 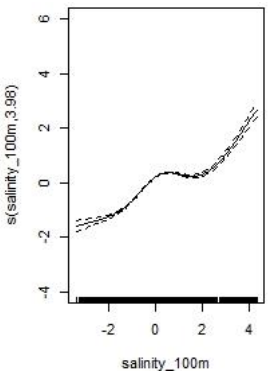

Fishing effort (longline)	MODEL 1	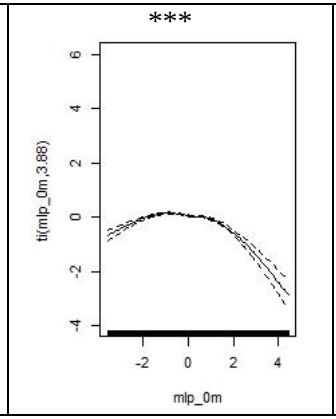	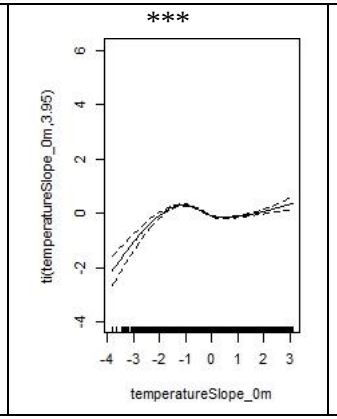	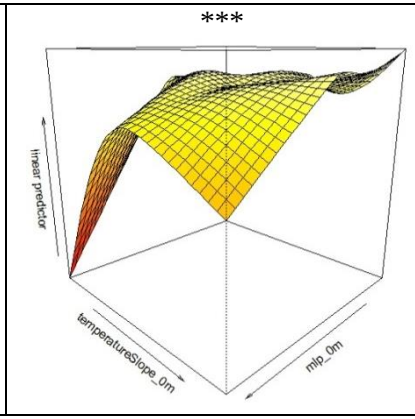	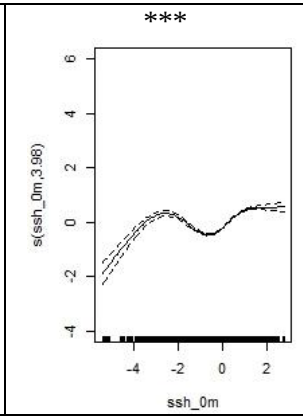	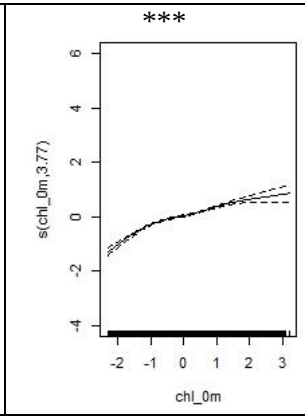	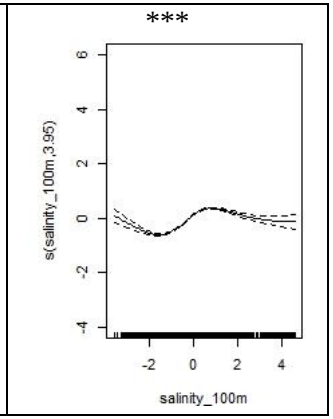

Extended Data Fig. 5. Estimated relationships between relative density of all sharks (top panel) and AIS fishing effort of all vessels (middle panels) and longlines only (bottom panels) with all environmental variables in the highest ranked (Model 1) of the generalised additive models (GAM) tested. Third column shows the interaction results between the two variables described in the first and second columns. Asterisks indicate significance level for each smooth term included in the GAM, representing $p < 0.001$ (***), < 0.01 (**).

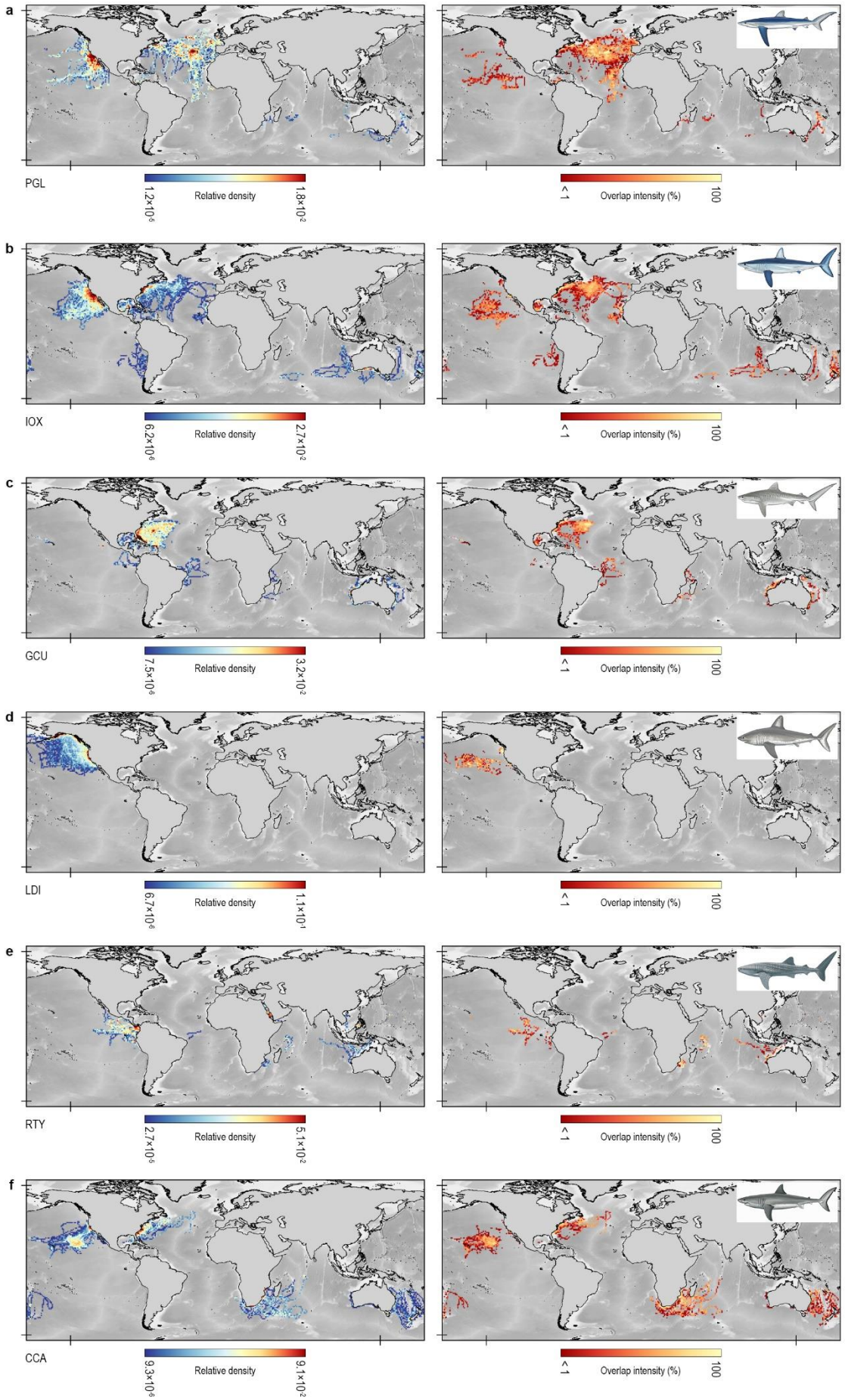
a
PGL
1.2×10⁻⁵
Relative density
1.8×10⁻²
< 1
Overlap intensity (%)
100
b
IOX
6.2×10⁻⁶
Relative density
2.7×10⁻²
< 1
Overlap intensity (%)
100
c
GCU
7.5×10⁻⁶
Relative density
3.2×10⁻²
< 1
Overlap intensity (%)
100
d
LDI
6.7×10⁻⁶
Relative density
1.1×10⁻¹
< 1
Overlap intensity (%)
100
e
RTY
2.7×10⁻⁵
Relative density
5.1×10⁻²
< 1
Overlap intensity (%)
100
f
CCA
9.3×10⁻⁶
Relative density
9.1×10⁻²
< 1
Overlap intensity (%)
100

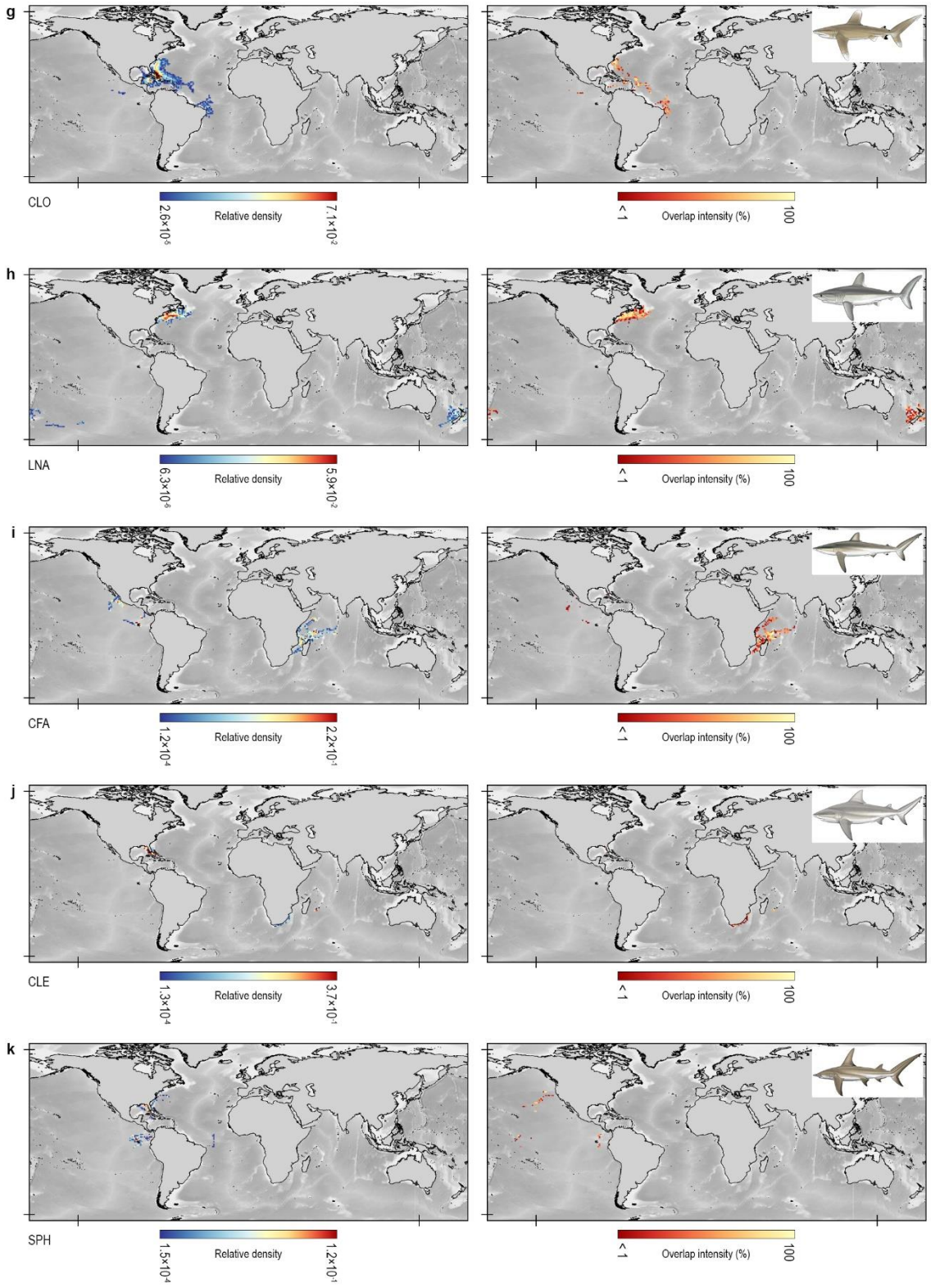

Extended Data Fig. 6. Relative density and spatial overlap intensity distributions for individual shark species. Relative density of sharks (left panels) tracked in 2002–2017 in comparison with shark-vessel spatial overlap intensity with AIS longline fishing vessels

(2012–2016) (right panels) for the 11 most data-rich species/taxa groups: (a) blue, *Prionace glauca*; (b) shortfin mako, *Isurus oxyrinchus*; (c) tiger, *Galeocerdo cuvier*; (d) salmon shark, *Lamna ditropis*; (e) whale shark, *Rhincodon typus*; (f) white, *Carcharodon carcharias*; (g) oceanic whitetip, *Carcharhinus longimanus*; (h) porbeagle, *Lamna nasus*; (i) silky, *Carcharhinus falciformis*; (j) bull, *Carcharhinus leucas*; and (k) hammerhead sharks, Sphyrna spp. (comprising: scalloped, *S. lewini*; great, *S. mokarran*; and smooth, *S. zygaena*). Shark images created by M. Dando.

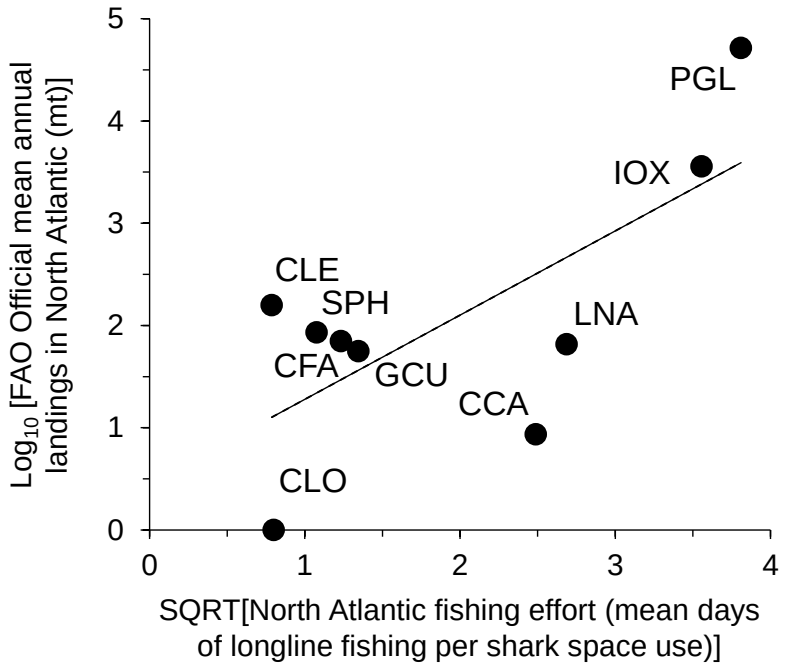

Extended Data Fig. 7. Relationship between North Atlantic fisheries' shark landings and AIS longline fishing effort in shark-vessel overlap areas. Plot showing shark landings from the North Atlantic (mean, 2012–2016) extracted from the Food and Agriculture Organization of the United Nations (FAO) total capture production database (see Methods) is dependent upon fishing effort of AIS longline vessels (2012–2016) in shark species space use areas in the North Atlantic (2002-2017). For linear regression analysis, we tested the null hypothesis (H_0) that $\beta = 0$ after normalising landings by log transformation and fishing effort by square-root transformation. We computed $r^2 = 0.51$, $F = 7.14$ and $F_{0.05(1),1,7} = 5.59$, therefore rejecting H_0 at the 5% level of significance with $p = 0.032$. Species identification codes are given in Fig. 1.

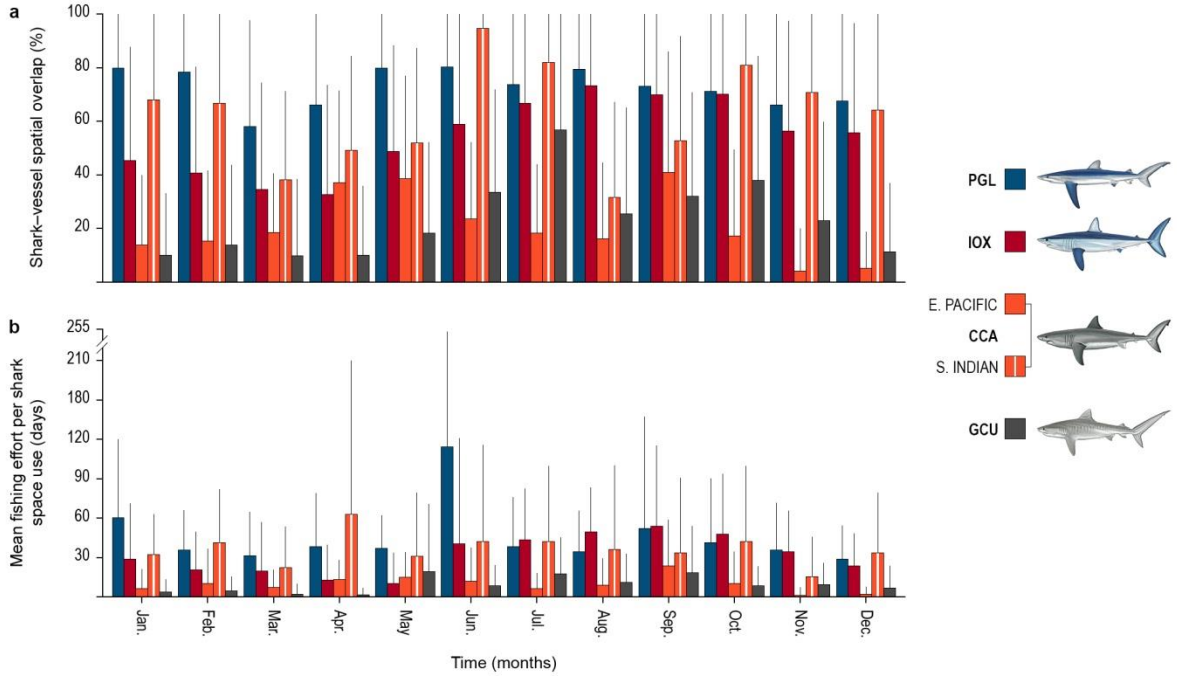

Extended Data Fig. 8. Example of temporal changes in spatial overlap and fishing effort. (**a**) Annual variation in shark-longline vessel spatial overlap and (**b**) longline fishing effort per shark space use. Shark species identification codes are given in Fig. 1. Error bars are ± 1 S.D. Shark images created by M. Dando.

a

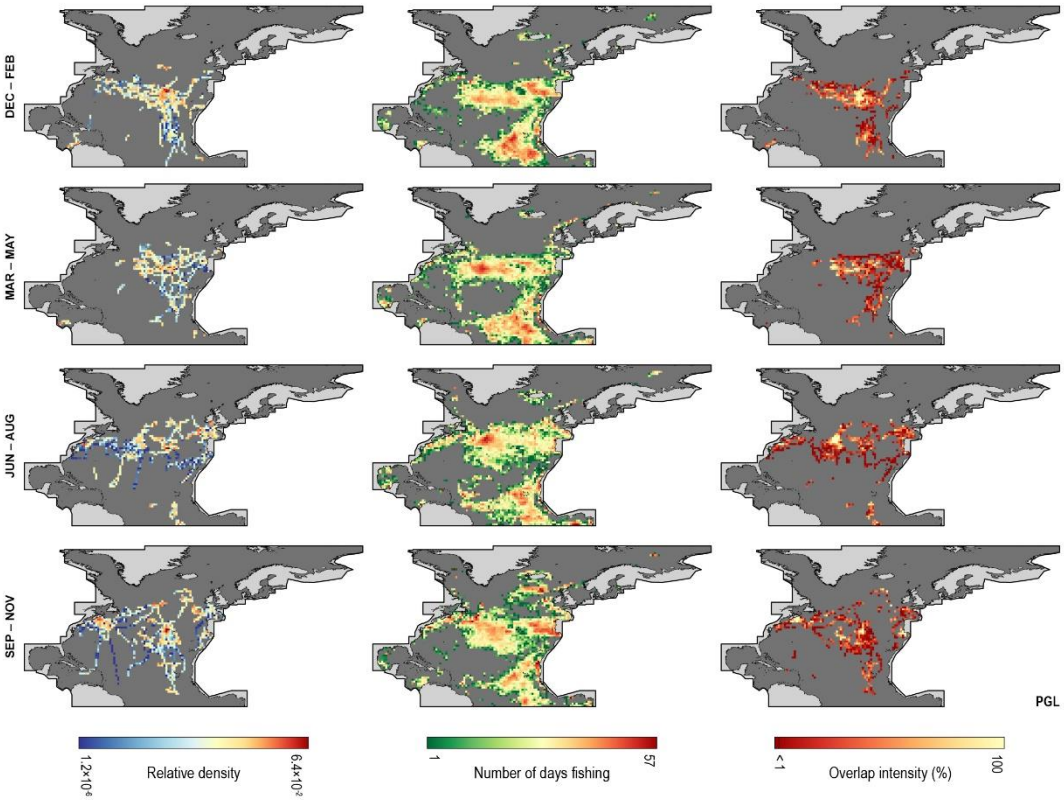
DEC – FEB
MAR – MAY
JUN – AUG
SEP – NOV
PGL
1.2×10⁶
Relative density
6.4×10²
1
Number of days fishing
57
<1
Overlap intensity (%)
100

b

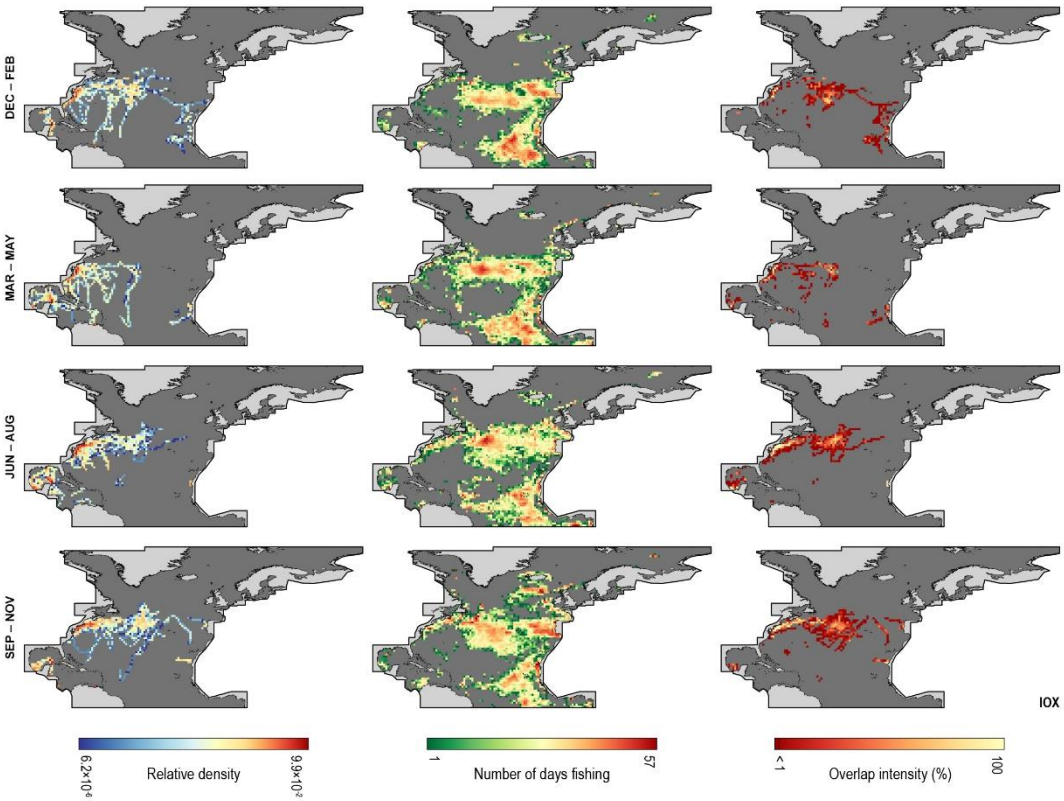
DEC – FEB
MAR – MAY
JUN – AUG
SEP – NOV
IOX
6.2×10⁶
Relative density
9.9×10²
1
Number of days fishing
57
<1
Overlap intensity (%)
100

c

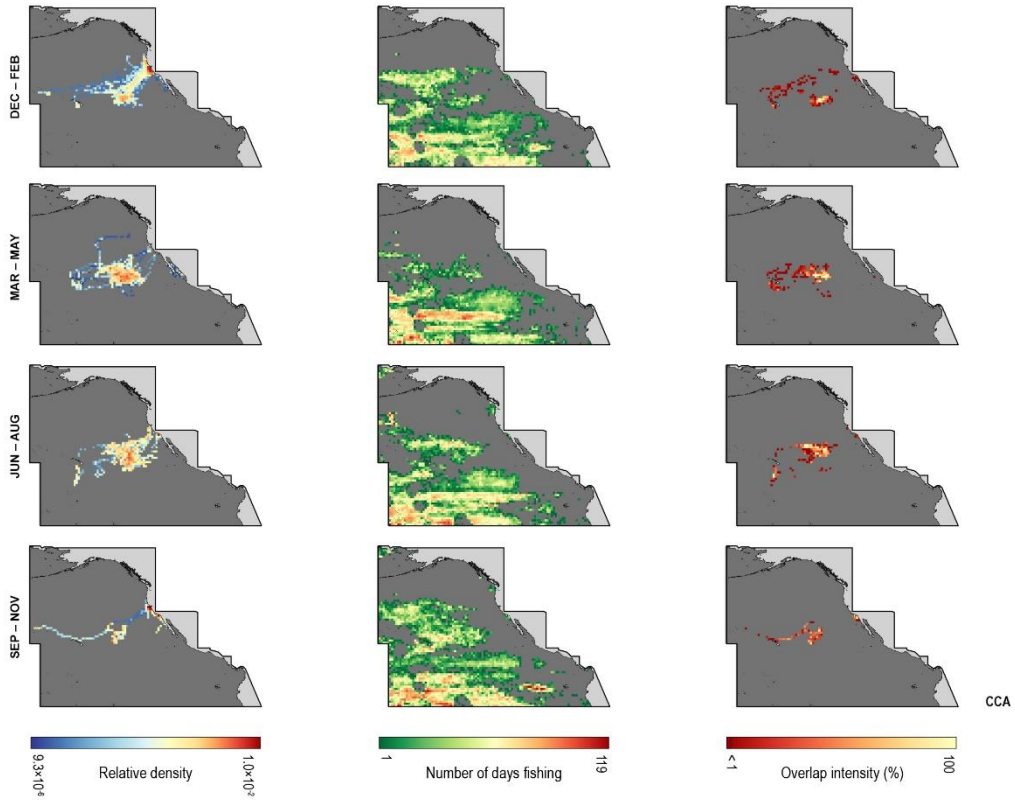
DEC – FEB
MAR – MAY
JUN – AUG
SEP – NOV
CCA
9.3×10⁻⁶
Relative density
1.0×10⁻²
1
Number of days fishing
119
<1
Overlap intensity (%)
100

d

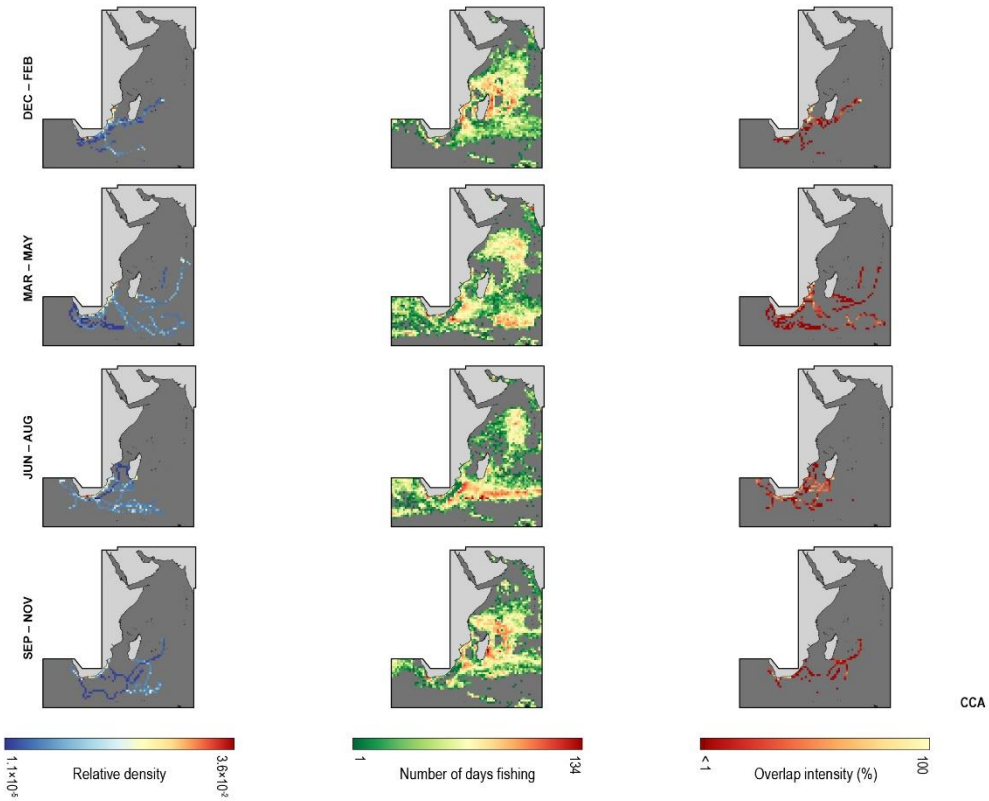
DEC – FEB
MAR – MAY
JUN – AUG
SEP – NOV
CCA
1.1×10⁻⁶
Relative density
3.6×10⁻³
1
Number of days fishing
134
<1
Overlap intensity (%)
100

e

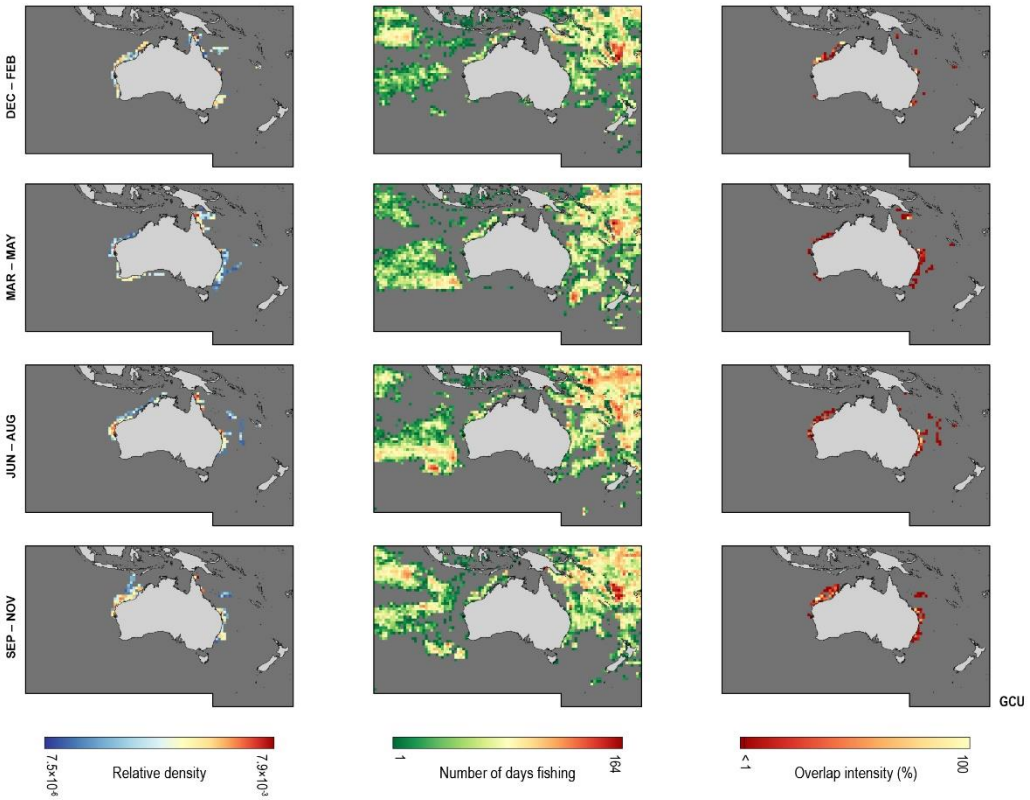

Extended Data Fig. 9. Seasonal shifts in sharks, longline vessels and shark-vessel overlap intensity. Relative spatial density of sharks (left panels), longline fishing effort (middle), and percentage spatial overlap intensity (right panels) in each seasonal quarter for (**a**) North Atlantic blue and (**b**) shortfin mako sharks, (**c**) east Pacific and (**d**) southwest Indian Ocean white sharks, and for (**e**) tiger sharks in the Oceania region. Shark species identification codes at bottom right of each panel are given in Fig. 1.

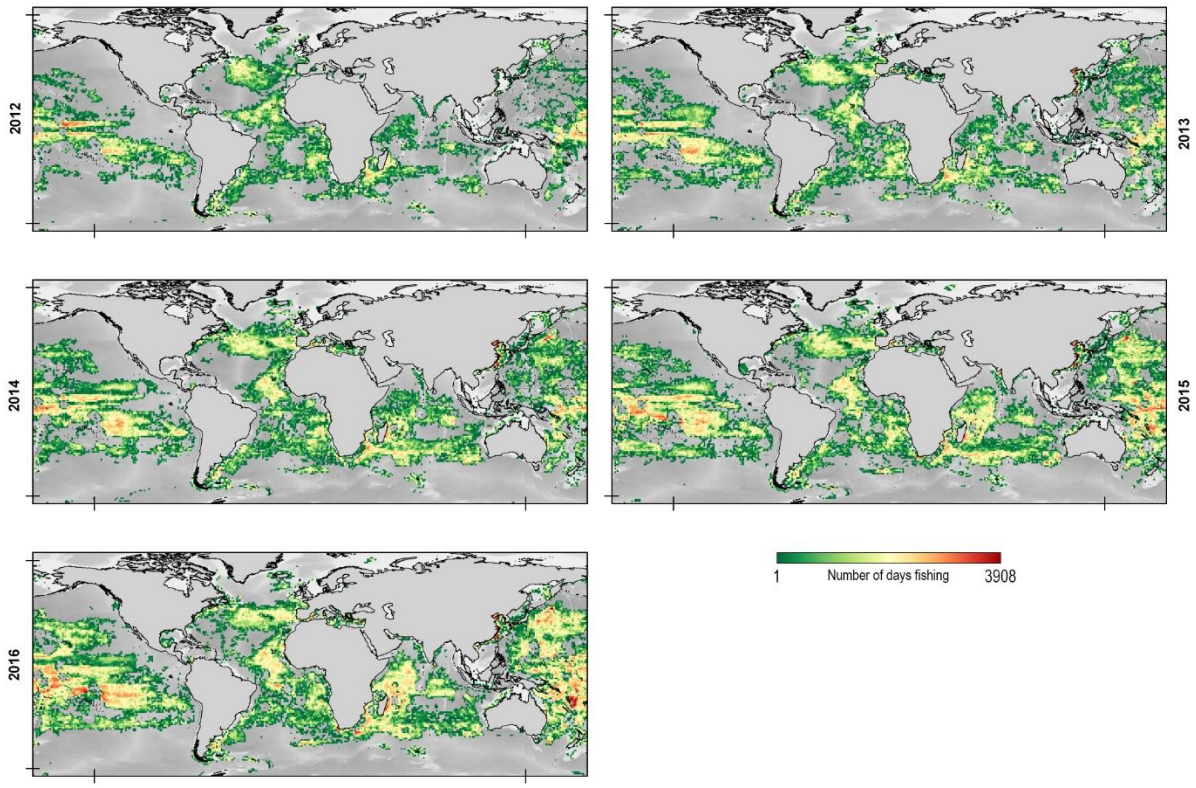

Extended Data Fig. 10. Annual spatial distribution of AIS longline fishing effort, 2012–2016. The global distribution of AIS monitored fishing effort varied across years as new AIS satellite receivers became operational which increases global coverage (for details see ref. 21). However, we calculated the mean annual fishing effort distribution across the 5 year period since the global spatial extent was broadly similar between years but also overlapped temporally with more years for which we had shark track data (2002–2017). The maximum fishing effort value observed per grid cell showed no increasing trend through time (max. value: 2012 = 291 fishing effort days; 2013 = 2337 d; 2014 = 1860 d; 2015 = 1749 d; 2016 = 3908 d) indicating a mean value taken across the 5 years was conservative and unlikely to lead to overestimates of fishing effort per shark space use (see Methods).